AMERICAN SOCIETY FOR MICROBIOLOGY | Molecular and Cellular Biology

# Evidence for Multiple Mediator Complexes in Yeast Independently Recruited by Activated Heat Shock Factor

**Jayamani Anandhakumar, Yara W. Moustafa, Surabhi Chowdhary, Amoldeep S. Kainth, David S. Gross**

Department of Biochemistry and Molecular Biology, Louisiana State University Health Sciences Center, Shreveport, Louisiana, USA

**Mediator is an evolutionarily conserved coactivator complex essential for RNA polymerase II transcription. Although it has been generally assumed that in *Saccharomyces cerevisiae*, Mediator is a stable trimodular complex, its structural state *in vivo* remains unclear. Using the "anchor away" (AA) technique to conditionally deplete select subunits within Mediator and its reversibly associated Cdk8 kinase module (CKM), we provide evidence that Mediator's tail module is highly dynamic and that a subcomplex consisting of Med2, Med3, and Med15 can be independently recruited to the regulatory regions of heat shock factor 1 (Hsf1)-activated genes. Fluorescence microscopy of a scaffold subunit (Med14)-anchored strain confirmed parallel cytoplasmic sequestration of core subunits located outside the tail triad. In addition, and contrary to current models, we provide evidence that Hsf1 can recruit the CKM independently of core Mediator and that core Mediator has a role in regulating postinitiation events. Collectively, our results suggest that yeast Mediator is not monolithic but potentially has a dynamic complexity heretofore unappreciated. Multiple species, including CKM-Mediator, the 21-subunit core complex, the Med2-Med3-Med15 tail triad, and the four-subunit CKM, can be independently recruited by activated Hsf1 to its target genes in AA strains.**

In all organisms, transcription represents the initial, and often most important, step in gene expression. In mammals, cell identity is established and maintained by the transcription of master identity genes driven by special regulatory elements known as superenhancers (1). Cell identity in the simple eukaryote *Saccharomyces cerevisiae* (budding yeast) is likewise governed by the transcription of master control genes, although here it is due to their translocation from a repressive to a permissive chromatin environment (reviewed in reference 2). Additionally, disease states such as cancer, diabetes, and neurodegeneration can arise from misregulated gene transcription (3). Pivotal to the expression of RNA polymerase II (Pol II) transcribed genes is the function of Mediator, an evolutionarily conserved protein complex that serves as a physical and functional bridge between gene-specific regulators and the general transcriptional machinery (GTM) (reviewed in references 4 to 7). Importantly, although Pol II itself is rarely (if ever) a direct target of DNA-bound transcription factors (TFs), Mediator is a frequent target (8–11). Mediator is also the target of loss-of-function mutations linked to a variety of human diseases, including cancer, infantile cerebral and cerebellar atrophy, DiGeorge syndrome, and congenital heart disease (reviewed in reference 12).

Biochemical, genetic, and structural studies have demonstrated that Mediator is organized into distinct head, middle, and tail modules. A fourth subcomplex, termed the Cdk8-kinase module (CKM), has been shown to reversibly associate with the core to form holo-Mediator and plays a regulatory role (reviewed in references 4 and 5). Holo-Mediator isolated from *S. cerevisiae* contains 25 subunits and has a molecular mass of ~1.5 MDa, with the core accounting for two-thirds of the total. The distinctive modular structure of Mediator (see Fig. 1A) contributes to its multiple layers of function. For example, the head module is assembled into a jawlike structure comprised of fixed (Med17-Med11-Med22) and movable jaws (the latter consisting of the C terminus of Med8 joined to the Med18-Med20 heterodimer) (13). The flexibility and extended shape of the head permit interactions with Pol II at three putative interaction surfaces—on Rpb1 (within its C-terminal domain [CTD]), Rpb3, and the Rpb4/Rpb7 subcomplex—as well as with other components of the transcription initiation complex, including TBP, TFIIB and TFIIH (13–18). In both yeast and humans, Med17 serves as the structural hub within the head module, as well as a major link between head and middle through its interaction with the scaffold subunit Med14 and the middle subunits Med7, Med10, and Med21 (19–21).

The eight tightly associated subunits of the middle module confer structural integrity on Mediator and also contact Pol II. Two—Med7 and Med21—serve a hinge function (22) critical to Mediator's ability to undergo structural rearrangements. The tail module harbors subunits that are frequently targeted by activators. For example, the conserved subunit Med15 serves as the target of the yeast activators Gcn4, Gal4, Oaf1, Pdr1/Pdr3, and Hsf1 (10, 23–27), as well as mammalian sterol regulatory element-binding protein (SREBP) (11). Med14, generally assigned to either the tail or middle, has recently been shown to serve as a central scaffold necessary for integrating the three separate modules of the core into a single functional entity (16, 19–21).

A model has been proposed whereby Mediator's binding to the GTM and transcription cofactors is linked to large-scale rearrangements in its structure that occur upon Mediator binding to the activation domains of gene-specific TFs (28–30; reviewed in

**Received** 4 January 2016 **Returned for modification** 4 February 2016
**Accepted** 4 May 2016

**Accepted manuscript posted online** 16 May 2016

**Citation** Anandhakumar J, Moustafa YW, Chowdhary S, Kainth AS, Gross DS. 2016. Evidence for multiple Mediator complexes in yeast independently recruited by activated heat shock factor. Mol Cell Biol 36:1943–1960. doi:10.1128/MCB.00005-16.

Address correspondence to David S. Gross, dgross@lsuhsc.edu.

J.A. and Y.W.M. contributed equally to this work.

Supplemental material for this article may be found at http://dx.doi.org/10.1128/MCB.00005-16.

Copyright © 2016, American Society for Microbiology. All Rights Reserved.

reference 5). These allosteric alterations occur at the interfaces between head, middle, and tail and facilitate assembly of the GTM into a functional transcription initiation complex (20). Additional roles for Mediator in regulating Pol II transcription, including its regulation of Pol II promoter escape, elongation rate, and processivity, have been described (31–33). These functions may likewise be dependent on activator-induced structural rearrangements.

Heat shock factor 1 (HSF1) is a sequence-specific activator that regulates the transcription of heat shock protein (*HSP*) genes that encode molecular chaperones and other cytoprotective proteins. HSF1 has been additionally implicated in promoting the oncogenic state of diverse human cancers through its ability to activate a novel set of genes (34–36). Interestingly, human heat shock factor 2 (HSF2) (a paralogue of HSF1) can functionally substitute for its yeast counterpart (37), underscoring the strong conservation of the protein. In yeast, Hsf1 is constitutively nuclear (38) although only a fraction is bound to chromatin and transcriptionally active in nonstressed cells (39–42). Following exposure to thermal stress (or other proteotoxic stimuli), inactive Hsf1 monomers trimerize and cooperatively bind to the remaining, lower-affinity heat shock elements (HSEs) in chromatin (43). DNA-bound Hsf1 then triggers the recruitment of Mediator and other coactivators (27, 44–48), culminating in the assembly of the Pol II initiation complex at *HSP* core promoters and transcription.

Most models of yeast Mediator have suggested that it is a monolithic, 21-subunit complex that reversibly associates with the CKM (16, 20, 21, 49). Studies using conventional mutants have identified the existence of subcomplexes (generally comprised of tail and scaffold subunits) whose existence has been inferred using both *in vivo* and cell-free assays (49–51). However, analysis of traditional genetic mutants can be confounded by indirect effects. Moreover, even at the permissive temperature, the *in vivo* state of such mutants is nonphysiological. To more rigorously define the nature of the Mediator complex recruited to *HSP* genes and its role in regulating *HSP* gene transcription, we conditionally depleted select Mediator subunits from the nucleus using the anchor away (AA) technique (52). By coupling this powerful genetic approach with genomic occupancy, expression, and subcellular localization assays, we found that multiple species of Mediator exist and can be independently recruited by Hsf1 to its target *HSP* genes in AA strains. Additionally, we found that core Mediator, but not the CKM, is essential for Hsf1-mediated transcription and that it plays a role in postinitiation events.

## MATERIALS AND METHODS

**Strain construction.** The anchor away recipient strain HHY212 (obtained from the European *S. cerevisiae* Archive for Functional Analysis [EUROSCARF]) was rendered Trp$^-$ Leu$^-$ via Cre-mediated excision of *loxP*-flanked *LEU2* and *TRP1* genes, generating strain YM100. To construct YM100 derivatives bearing the desired FRB protein domain-tagged gene for use in the anchor away procedure (52), integrating cassettes were generated by PCR using as templates pFA6a-FRB-KanMX6 or pFA6a-FRB-His3MX6, encoding the FRB tag, and either *KAN-MX* or *HIS3-MX* as a selectable marker. Myc9-tagged derivatives of anchor away strains were constructed using a similar integrative transformation strategy. Plasmid pWZV87 (53) (a gift from K. Nasmyth), containing the Mycx9 tag and the *KlTRP1* selectable marker, was used as a template in the PCR amplification. FRB-green fluorescent protein (GFP)- and mCherry-tagged strains were made similarly, employing plasmids pFA6a-FRB-GFP-*KanMX6* and pFA6A-link-mCherry-*CaURA3*, respectively, as templates (gifts from D. Pincus and K. Tatchell, respectively). All tagged strains were confirmed using genomic PCR. The strains used in this study are listed in Table 1, and their growth phenotypes are evaluated in Fig. 2B and in Fig. S1 in the supplemental material.

**TABLE 1** Yeast strains

| Name | Genotype | Source or reference |
|---|---|---|
| HHY212 | *MATa tor1-1 fpr1::loxP-LEU2-loxP RPL13A-2×FKBP12::loxP-TRP1-loxP ade2-1 trp1-1 can1-100 leu2-3,112 his3-11,15 ura3-1* | 52 |
| YM100 | HHY212; *LEU2* and *TRP1* excised with Cre recombinase | This study |
| YM101 | HHY212; *MED14-FRB::KAN-MX* | This study |
| YM102 | HHY212; *MED7-FRB::KAN-MX* | This study |
| YM103 | YM100; *MED14-FRB::KAN-MX* | This study |
| YM104 | YM100; *MED7-FRB::KAN-MX* | This study |
| YM105 | YM103; *MED20-MYCx9::TRP1* | This study |
| YM106 | YM103; *MED31-MYCx9::TRP1* | This study |
| YM107 | YM103; *MED16-MYCx9::TRP1* | This study |
| YM108 | YM103; *SPT3-MYCx9::TRP1* | This study |
| YM109 | YM103; *TAF1-MYCx9::TRP1* | This study |
| YM111 | YM104; *MED20-MYCx9::TRP1* | This study |
| YM112 | YM103; *MED12-MYCx9::TRP1* | This study |
| YM113 | YM103; *MED13-MYCx9::TRP1* | This study |
| YM114 | YM100; *CDK8-FRB::HIS3* | This study |
| YM115 | YM114; *MED12-MYCx9::TRP1* | This study |
| YM116 | HHY212; *MED15-FRB::HIS3* | This study |
| YM117 | YM116; *LEU2* and *TRP1* excised with Cre recombinase | This study |
| YM118 | YM117; *SPT3-MYCx9::TRP1* | This study |
| YM119 | YM117; *CDK8-Mycx9::TRP1* | This study |
| YM120 | HHY212; *SPT20-FRB::HIS3* | This study |
| YM123 | YM103; *CDK8-MYCx9::TRP1* | This study |
| YM124 | HHY212; *MED16-FRB::KAN-MX* | This study |
| YM125 | YM117; *MED16-MYCx9::TRP1* | This study |
| YM126 | YM124; *LEU2* and *TRP1* excised with Cre recombinase | This study |
| ASK201 | YM103; *MED15-MYCx9::TRP1* | This study |
| ASK202 | YM104; *MED15-MYCx9::TRP1* | This study |
| ASK203 | YM126; *MED15-MYCx9::TRP1* | This study |
| AJ101 | YM103; *MED2-MYCx9::TRP1* | This study |
| AJ102 | YM103; *MED3-MYCx9::TRP1* | This study |
| AJ103 | YM103; *MED5-MYCx9::TRP1* | This study |
| AJ126 | YM117; *MED2-MYCx9::TRP1* | This study |
| AJ127 | YM117; *MED3-MYCx9::TRP1* | This study |
| AJ128 | YM117; *MED5-MYCx9::TRP1* | This study |
| AJ201 | HHY212; *MED14-FRB-GFP::KAN-MX* | This study |
| AJ202 | AJ201; *MED15-mCherry::URA3* | This study |
| AJ203 | AJ201; *MED16-mCherry::URA3* | This study |
| AJ204 | AJ201; *MED18-mCherry::URA3* | This study |
| AJ205 | AJ201; *MED2-mCherry::URA3* | This study |
| BY4742-HSF1-AA | *MATα tor1-1 fpr1Δ RPL13A-FKBP12::NAT-MX HSF1-FRB-yEGFP::KAN-MX lys2Δ ura3Δ his3Δ leu2Δ* | F. Holstege |

**Cultivation, heat shock, and rapamycin induction conditions.** *S. cerevisiae* strains were cultivated at 30°C to early log phase ($A_{600}$ = 0.4 to 0.7) in rich broth supplemented with 0.02 mg/ml adenine (YPDA). Heat shock induction was achieved by an instantaneous temperature shift fom 30°C to 39°C through addition of an equal volume of prewarmed YPDA medium (50°C) to the culture. The cultures were shaken vigorously in a 39°C water bath for the lengths of time indicated in the figure legends. To terminate heat shock induction, formaldehyde (HCHO) was added to a

final concentration of 1% (chromatin immunoprecipitation [ChIP]) or sodium azide was added to a final concentration of 20 mM (reverse transcription-quantitative PCR [RT-qPCR]). For anchor away experiments, cultures were incubated in the presence of 1 μg/ml rapamycin for various lengths of time at 30°C prior to heat shock induction, whose duration is indicated in the figures. Rapamycin was purchased from Tecoland Corporation, Irvine, CA, or LC Laboratories, Woburn, MA, and stored as a 1-mg/ml concentrated stock in 100% ethanol at −20°C.

**Spot dilution analysis.** Cells were grown to stationary phase in rich YPDA medium and then diluted to a uniform cell density ($A_{600}$ = 0.5) and transferred to a 96-well microtiter dish. Each sample was then serially 5-fold diluted using double-distilled water and applied to solid YPDA medium or YPDA medium with rapamycin (1 μg/ml), using a 48-prong stainless steel applicator or by manually pipetting 6 μl. Cells were grown at the temperatures and for the durations indicated in Fig. 2B and Fig. S1 in the supplemental material.

**ChIP.** ChIP experiments were performed as previously described (27), except as noted below. Mid-log-phase cultures (typically 500 ml) were used in both rapamycin and heat shock time course experiments; 50-ml aliquots were removed at each time point, to which formaldehyde was added to a final concentration of 1%. Cells were harvested, washed, and resuspended in 250 μl lysis buffer and lysed with vigorous shaking in the presence of glass beads (~300 mg) at 4°C for 30 min. The cell lysates were then transferred to 1.5-ml TPX tubes and sonicated at 4°C using a Diagenode Biorupter Plus (40 cycles with 30-s pulses). This procedure generates chromatin fragments with a mean size of ~250 to 350 bp. The TPX tubes were centrifuged to clarify the supernatants; these were then brought up to 2,000 μl using ChIP lysis buffer. To perform immunoprecipitation, the equivalent of 500 to 800 μg chromatin protein (typically 200 to 400 μl) was incubated with one of the following antibodies: 1 μl of anti-Hsf1 (raised in our laboratory [54]); 2.5 μl of anti-Myc (Santa Cruz Biotechnology); 1 to 2 μl of anti-FRB (Enzo Life Sciences; ALX-215-065-1); 1 μl of anti-H3 globular domain (Abcam; ab1791); 1.5 μl of anti-Srb4/Med17, anti-Srb8/Med12, or anti-Srb7/Med21 (gifts from Richard A. Young, Whitehead Institute/Massachusetts Institute of Technology); 1 μl of anti-Rgr1/Med14 (a gift from Steve Hahn, Fred Hutchinson Cancer Research Center); 0.75 μl of anti-Gal11/Med15 (a gift from Mark Ptashne, Sloan Kettering Institute); and 1 to 1.5 μl of anti-Pol II (Rpb1 C-terminal domain; raised in our laboratory [55]).

Immunoprecipitated DNA was resuspended in 60 μl sterile water; 2 μl was used in qPCR with $RT^2$ qPCR SYBR green/ROX master mix (SABiosciences; 330529) on an Applied Biosystems 7900HT real-time PCR system. The DNA was quantified using a standard curve specific for each amplicon, and background signal arising from the beads alone was subtracted. For Mediator subunit ChIP, background was determined by signal arising from incubating an equivalent volume of chromatin extract with protein A Sepharose beads (GE Healthcare; catalog no. 17-0963-03). For FRB- and Myc-ChIPs, background was determined by immunoprecipitating an equivalent amount of chromatin isolated from the parental, nontagged strain (HHY212 or YM100) using anti-FRB or anti-Myc antibody (Ab). In certain cases, the Myc/FRB ChIP background was determined through use of protein G Sepharose beads alone (GE Healthcare; catalog no. 17-0618-02). For Hsf1 and Pol II ChIPs, the signal obtained from immunoprecipitating an equivalent amount of chromatin using preimmune serum was used as the background. To normalize for variation in the yield of chromatin extracts, input chromatin was used. Briefly, 32 μl was removed from the 2,000-μl chromatin lysate isolated as described above, and the volume was brought up to 400 μl. HCHO-induced cross-links were reversed and DNA was deproteinized as for ChIP samples. The purified input DNA was dissolved in 240 μl Tris-EDTA (TE), and 2 μl was removed for qPCR. The signal arising from this represented 2% of the total input chromatin. The amplicons used for detection and quantification of genomic loci in ChIP and input DNAs are listed in Table 2.

**RT-qPCR.** Cells were cultivated in 600- to 650-ml mid-log-phase cultures, and 50-ml aliquots were removed for each heat shock time point and treated with 1/100 volume of 2 M sodium azide to terminate transcription. Total RNA was isolated using an RNeasy kit (Qiagen; 74204). Purified RNA (0.5 μg) and random primers were used in each cDNA synthesis using the High-Capacity cDNA reverse transcription kit (Applied Biosystems; 4368814). The synthesized cDNA was diluted 1:20, and 5 μl of diluted cDNA was added to each 20-μl real-time PCR mixture. Relative cDNA levels were quantified by the $\Delta\Delta C_t$ method (56). The Pol III transcript *SCR1* was used as a normalization control for quantification of *HSP* mRNA levels. The amplicons used for detection of cDNAs were as follows (the coordinates are relative to ATG): *SSA4*, +815 to +946; *HSP82*, +2134 to +2228; *HSP104*, +1646 to +1799; *ZPR1*, +720 to +809; *HSP12*, +9 to +133; *CTT1*, +193 to +314; and *PGM2*, +914 to +1038.

**Subcellular localization analysis.** For live-cell imaging, cells bearing the Med14-FRB-GFP-tagged gene were cultivated at 30°C to early log phase in synthetic complete (SC) growth medium supplemented with 0.1 mg/ml adenine. At various times after addition of rapamycin to 1 μg/ml, cells were collected by centrifugation of 1 to 1.5 ml of culture; 1 μl of the cell pellet was placed onto a pad of 2% agarose in SC medium containing 2 μg/ml rapamycin and maintained at 25°C. It was imaged on an Olympus fluorescence microscope with a UPlanFl 100×/1.3-numerical-aperature (NA) objective using a CoolSnap HQ charge-coupled-device camera. For imaging GFP, a 41001 filter set was used (Chroma Technology). For imaging mCherry, a TRITIC filter set (Olympus) was used. To control camera acquisition and the Z axis stepping motor (Ludl Electronic Products), we used Slidebook version 4 software (Intelligent Imaging Innovations). Fluorescence images (binned 2 by 2) were acquired in a single plane.

## RESULTS

**Mediator is recruited to the upstream regulatory regions of heat shock-induced *HSP* genes.** Previous work demonstrated the rapid, robust recruitment of Mediator to Hsf1-regulated genes in response to heat shock (27, 44). Given that the genomic regions with which Mediator associates in its global regulatory role are controversial and may be gene dependent (57–61), we wished to more precisely map where this recruitment takes place. We therefore amplified tandem intervals of four representative *HSP* genes—*HSP82*, *HSP104*, *SSA4*, and *ZPR1*—in a ChIP-qPCR analysis. We found that in acutely (5-min) heat-shocked cells, subunits from head (Med17), scaffold (Med14), and tail (Med15) prominently localized to the upstream activation sequence (UAS) and, to a lesser degree, the promoter of each of the four genes (Fig. 1B). The CKM subunits Cdk8, Med12, and Med13 likewise appeared to localize to the same regions, although their occupancy was less robust (data not shown), which may reflect reduced or less stable interaction, epitope accessibility, avidity of the antibodies, or a combination of all three. Detection of low ChIP signals for core subunits within *HSP* coding regions may reflect bona fide *in vivo* occupancy; it is also possible that they arise from hyper-ChIP-ability of actively transcribed chromatin domains (60, 62, 63). In contrast to Mediator, Pol II occupancy (Fig. 1B, purple bars) was prominent within both the promoters and the coding regions of these genes, consistent with their active transcriptional state.

**Cytoplasmic anchoring of Med14 severely reduces the abundance of most core subunits at induced *HSP* promoters, while recruitment of a tail subcomplex persists.** To gain a more complete understanding of the role played by Mediator in *HSP* gene regulation, we conditionally depleted subunits representative of each of its structural modules using the "anchor away" (AA) system developed by Haruki and colleagues (52). This was done by

**TABLE 2** Primers used in ChIP-qPCR

| ChIP amplification primer | Sequence |
|---|---|
| SSA4_UAS_F (−374 to −353) | 5′ GCC GCA CAT CCA TTC CGG TAT G 3′ |
| SSA4_UAS_R (−312 to −291) | 5′ CGG GCA AAA GAT ATC CGC TTT G 3′ |
| SSA4_PROM_F (−163 to −136) | 5′ GAC GAC AGT AAC AAA ATG TTC GT 3′ |
| SSA4_PROM_R (−115 to −93) | 5′ CCT CTG AAA AGT CCT TTA TTG GC 3′ |
| SSA4_5′ORF_F (+89 to +111) | 5′ ACT GTA TTA TGT GGG TTC ATC GC 3′ |
| SSA4_5′ORF_R (+171 to +194) | 5′ ATC AAG GTA ATA GAA CGA CGC C 3′ |
| SSA4_MID_ORF_F (+816 to +837) | 5′ GTC TTC GTC TGC TCA GAC ATC 3′ |
| SSA4_MID_ORF_R (+925 to +946) | 5′ CCA CTG GCT CCA ATG TAG ATC 3′ |
| SSA4_3′UTR_F (+1879 to +1900) | 5′ GGC CCC ACT GGA GCA CCA GAC 3′ |
| SSA4_3′UTR_R (+2016 to +2038) | 5′ CAT TTG CTA ATT ACT GAT TGT G 3′ |
| HSP82_UAS_F (−303 to −278) | 5′ GTC ACA TAT TGT TCG AAC AAT TCT GG 3′ |
| HSP82_UAS_R (−238 to −263) | 5′ CTT CCA CGG CGT TCT AGA AAA AAA AG 3′ |
| HSP82_PROM1_F (−157 to −140) | 5′ TCC GCC ACC CCC TAA AAC 3′ |
| HSP82_PROM1_R (−113 to −88) | 5′ TGA GGA GGT CAC AGA TGT TAA GAA TT 3′ |
| HSP82_PROM2_F (−233 to −217) | 5′ CTA GAA CGC CGT GGA AG 3′ |
| HSP82_PROM2_R (−129 to −110) | 5′ GAA TTG AAG GGA TAA GCT GC 3′ |
| HSP82_5′ORF_F (+599 to +622) | 5′ TCG TGG CCT ACC CAA TCC AAT TAG 3′ |
| HSP82_5′ORF_R (+694 to +717) | 5′ GTC GTC TTC ATC CTT CTT TTC CTC 3′ |
| HSP82_MID_ORF_F (+1248 to +1274) | 5′ GTT CTA CTC GGC TTT CTC CAA AAA TAT 3′ |
| HSP82_MID_ORF_R (+1419 to +1444) | 5′ CAG CCT TTA GAG ATT CAC CAG TGA TG 3′ |
| HSP82_3′UTR_F (+2134 to +2158) | 5′ AAC ATC ATG GCC TTG AAT AGG TTA T 3′ |
| HSP82_3′UTR_R (+2203 to +2228) | 5′ CAT GCA GAT GCC CTA TTT ACA TAC TT 3′ |
| HSP104_UAS_F (−267 to −247) | 5′ CTT AAA CGT TCC ATA AGG GGC 3′ |
| HSP104_UAS_R (−216 to −196) | 5′ TGC AGT TCT TTG AGA TGG GCC 3′ |
| HSP104_PROM_F (−130 to −107) | 5′ GCA TTG TAA TCT TGC CTC AAT TCC 3′ |
| HSP104_PROM_R (−70 to −92) | 5′ GTT ATT GCT GAT TCG ATT CAA GG 3′ |
| HSP104_MID_ORF_F (+1646 to +1669) | 5′ CAG CTG CAA GAT TGA CTG GTA TCC 3′ |
| HSP104_MID_ORF_R (+1777 to +1799) | 5′ CCT GAT CTA GAC AAT CTA ACG GC 3′ |
| HSP104_3′UTR_F (+2612 to +2631) | 5′ GGA AGC TGA AGA ATG TCT GG 3′ |
| HSP104_3′UTR_R (+2699 to +2718) | 5′ GTC ATC ATC AAT TTC CAT AC 3′ |
| ZPR1_UAS_F (−299 to −278) | 5′ GGC ATC GAG TGA ATT TTT CAC C 3′ |
| ZPR1_UAS_R (−238 to −217) | 5′ GAA AAC TCC AGA GGG TTT CGG C 3′ |
| ZPR1_PROM_F (−131 to −107) | 5′ AAT GCT ATG ATG TTC AAC GCA AAG G 3′ |
| ZPR1_PROM_R (−96 to −74) | 5′ ACG ATG CGA ACC TAC CCG ATA AC 3′ |
| ZPR1_MID_ORF_F (+720 to +739) | 5′ GAC CAG TTG GAG CAA CGT CG 3′ |
| ZPR1_MID_ORF_R (+791 to +809) | 5′ GCT GAG CCA ACT TTG ACA G 3′ |
| ZPR1_3′UTR_F (+1451 to +1470) | 5′ GGT TGA GTA ACG ATC GTT GG 3′ |
| ZPR1_3′UTR_R (+1515 to +1533) | 5′ GAG TGC TTG TGT GGT TAG G 3′ |

C-terminally tagging such subunits with the FRB domain of human mTOR in a yeast strain expressing the ribosomal protein RPL13A fused to FKBP12 (a 12-kDa human FK506-binding protein). Conditional depletion of FRB-tagged proteins occurs upon exposure of such cells to rapamycin, which induces a strong interaction between FRB and FKBP12. RPL13A is actively imported into the nucleus, where it is assembled into the 60S ribosomal subunit, followed by its export back into the cytoplasm (see Fig. 2A for the AA scheme). The FKBP12 fusion, along with other genetic modifications that render these strains immune to the toxic effect of rapamycin, have been previously described (52).

We initially investigated the role of Med14, given that it serves as a physical and functional scaffold connecting the head, middle, and tail modules (16, 19–21), as well as previous indications that it governs *HSP* gene expression through its influence on Hsf1 binding and Pol II recruitment and postrecruitment steps (27, 31, 38). The Med14 AA strain grew normally on rich medium at 15°C, 30°C, and 37°C, while as expected its growth was strongly inhibited on medium containing rapamycin (Fig. 2B). (Other strains constructed for this study were similarly tested for growth phenotypes [see Fig. S1 in the supplemental material].) Addition of rapamycin to liquid cultures triggered substantial depletion of Med14-FRB from nuclei within 30 min, as suggested by ChIP analysis of representative *HSP* genes in cells subjected to a subsequent acute heat shock (Fig. 2C). Longer rapamycin preincubations induced further depletion, resulting in >90% reduction in Med14 occupancy. Therefore, despite its central architectural role, Med14 can be efficiently depleted from yeast nuclei using the anchor away system.

How Mediator is assembled into the 21-subunit core complex is unknown, but we reasoned that since Med14 serves as a scaffold bridging all three core modules, depletion of Med14-FRB might result in the concomitant depletion of physically associated subunits in the head, middle, and tail. Additionally, as the CKM has been shown to interact with the core complex through the middle module (64), CKM recruitment, too, may be affected by Med14 depletion. Consistent with these expectations, ChIP analysis of induced *HSP* genes revealed that head (Med17 and Med20) and middle (Med21 and Med31) subunits were depleted in a progressive fashion that paralleled loss of Med14-FRB over the rapamycin

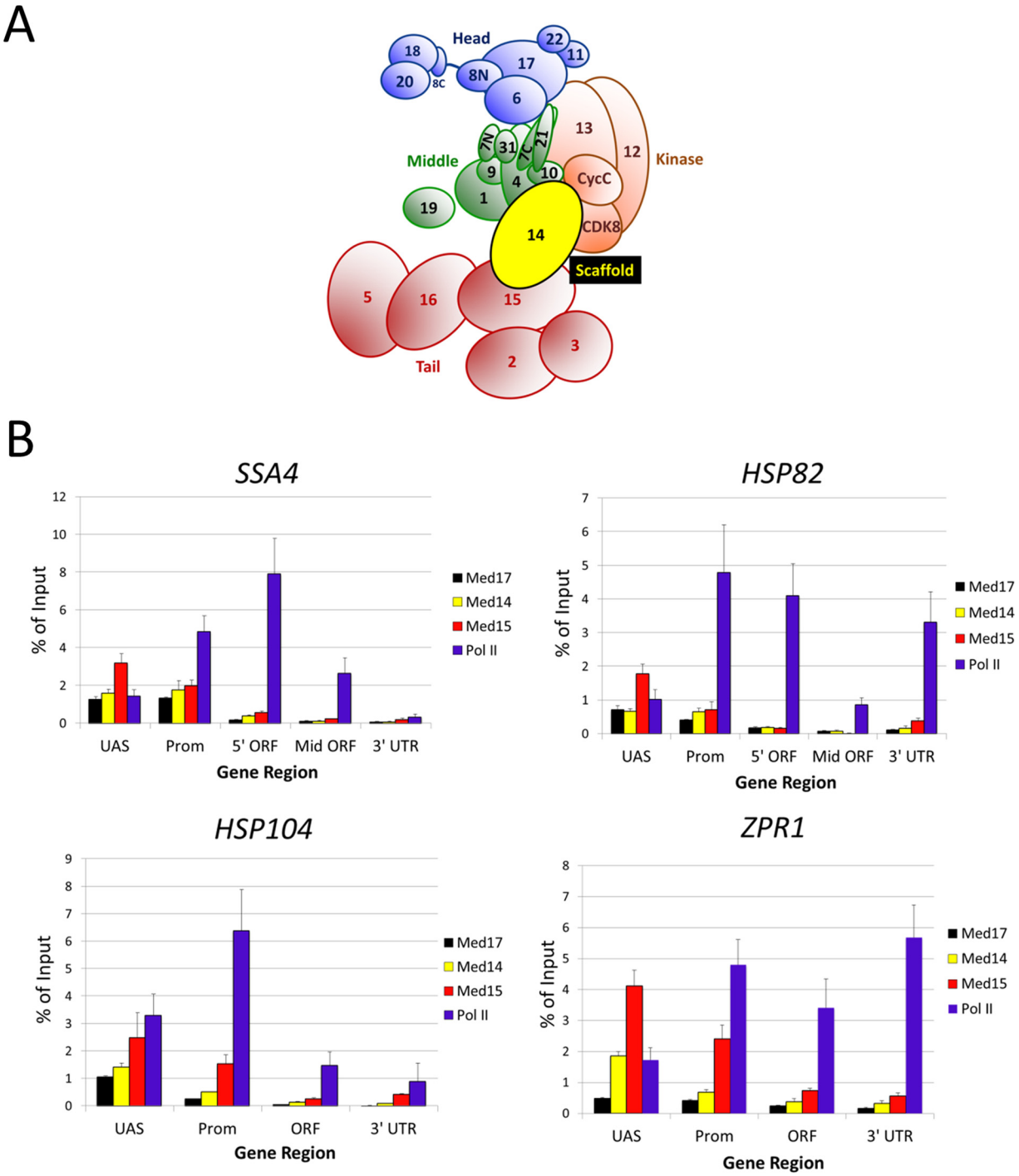


**FIG 1** Yeast Mediator and its location within *HSP* genes following acute heat shock. (A) Yeast Mediator subunit arrangement and modular structure, canonical view. The schematic illustrates a current model of *S. cerevisiae* core Mediator and the reversibly associated Cdk8-kinase module. The model is based on both structural analyses and protein-protein interaction assays (20, 22, 72, 73). (Adapted from reference 69 and used with permission.) (B) ChIP analysis of Pol II and representative head (Med17), tail (Med15), and scaffold (Med14) subunits of core Mediator at four Hsf1-regulated genes. Yeast cells were subjected to a 5-min, 39°C heat shock prior to fixation with 1% formaldehyde. Chromatin was isolated and sonicated as described in Materials and Methods. Antisera raised against recombinant proteins were used to detect Mediator subunits; antiserum raised against the CTD of Rpb1 was used to detect Pol II. Shown is the occupancy of each factor normalized to input. The data are shown as means and standard deviations (SD) of 2 or 3 independent biological replicates ($n = 4$ for Pol II). The midpoint coordinates of qPCR amplicons used in this analysis, presented relative to the ATG start codon (+1), are as follows: *SSA4* UAS (−333), Prom (promoter) (−128), 5′ open reading frame (ORF) (+142), mid-ORF (+881), and 3′ untranslated region (UTR) (+1959); *HSP82* UAS (−283), Prom (−123), 5′ ORF (+658), mid-ORF (+1346), and 3′ UTR (+2181); *HSP104* UAS (−232), Prom (−111), ORF (+1723), and 3′ UTR (+2665); and *ZPR1* UAS (−258), Prom (−103), ORF (+765), and 3′ UTR (+1492).

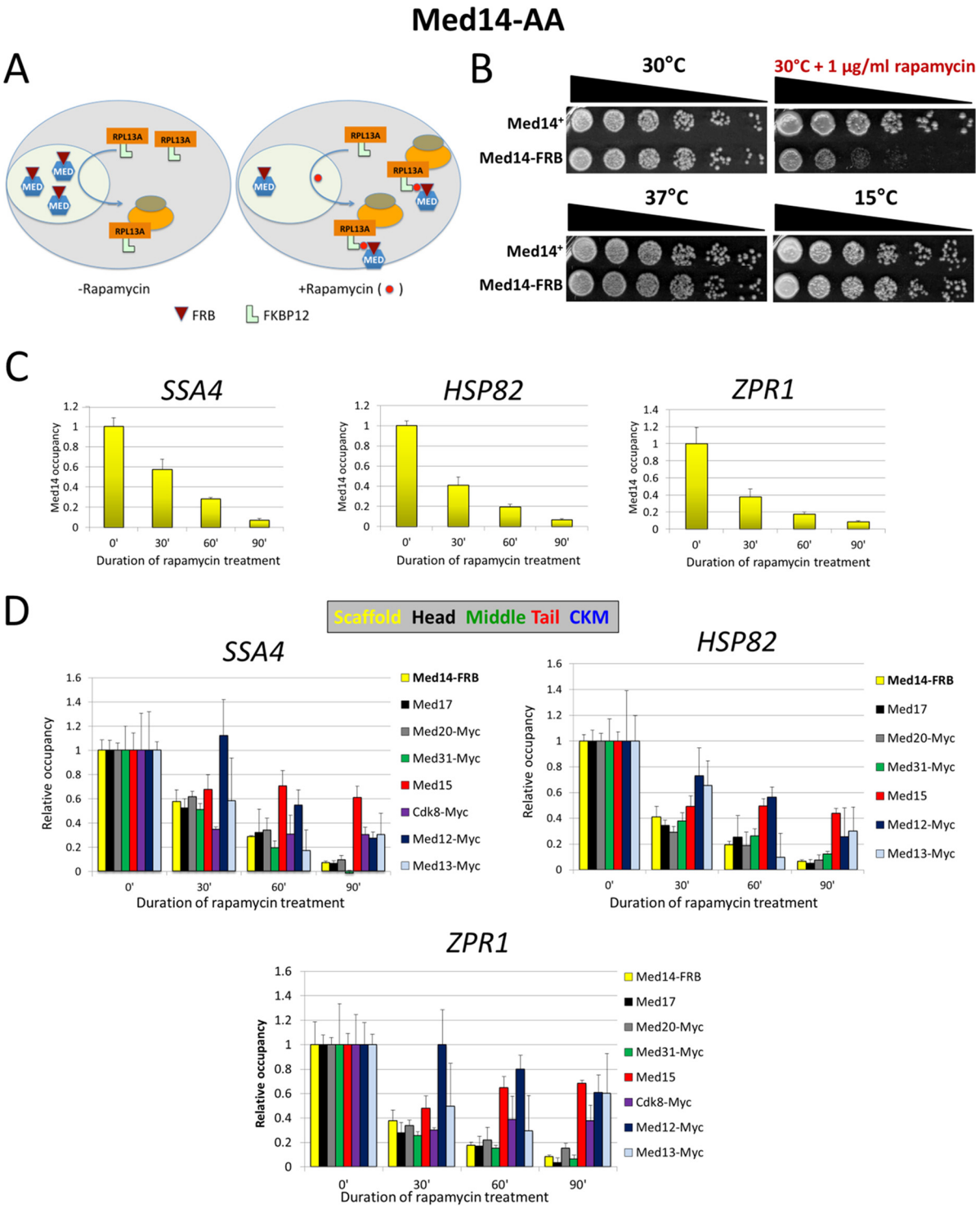


**FIG 2** Heat shock-activated UAS/promoter regions in cells exposed to rapamycin are efficiently depleted of Med14-FRB, and the abundance of most, but not all, core subunits is reduced in parallel. (A) Anchor away technique (52). See the text for details. (B) Spot dilution analysis of parental (Med14$^{+}$) and Med14-FRB AA strains (HHY212 and YM101, respectively). Depicted are 5-fold serial dilutions spotted onto YPDA medium supplemented with drug as indicated. The plates were incubated at 30° or 37°C for 2 to 3 days and at 15°C for 7 days. (C) ChIP analysis of Med14-FRB at *SSA4*, *HSP82*, and *ZPR1* UAS/promoter regions in YM101 cells subjected to treatment with 1 μg/ml rapamycin for the indicated times, followed by a 5-min heat shock. ChIP was performed as in Fig. 1B. Med14 was detected with anti-Rgr1/Med14 antiserum, and its abundance is presented relative to that seen in nontreated cells similarly subjected to a 5-min heat shock (0′). Depicted are means and SD; $n = 2$. (D) ChIP analysis of representative Mediator subunits conducted and quantified as in panel C. Antibodies raised against recombinant proteins were used to detect Mediator subunits lacking a C-terminal Myc tag; those containing one were detected with an anti-Myc monoclonal antibody. For both panels C and D, mock IP signal (beads alone for Med14, Med15, Med17, and Med21; anti-Myc IP of chromatin isolated from the corresponding parental strain for the Myc-tagged subunits) was subtracted from each ChIP signal prior to normalization. Depicted are means and SD; $n = 2$ or 3. The strains used were YM103, YM105, YM106, YM112, YM113, and YM123.

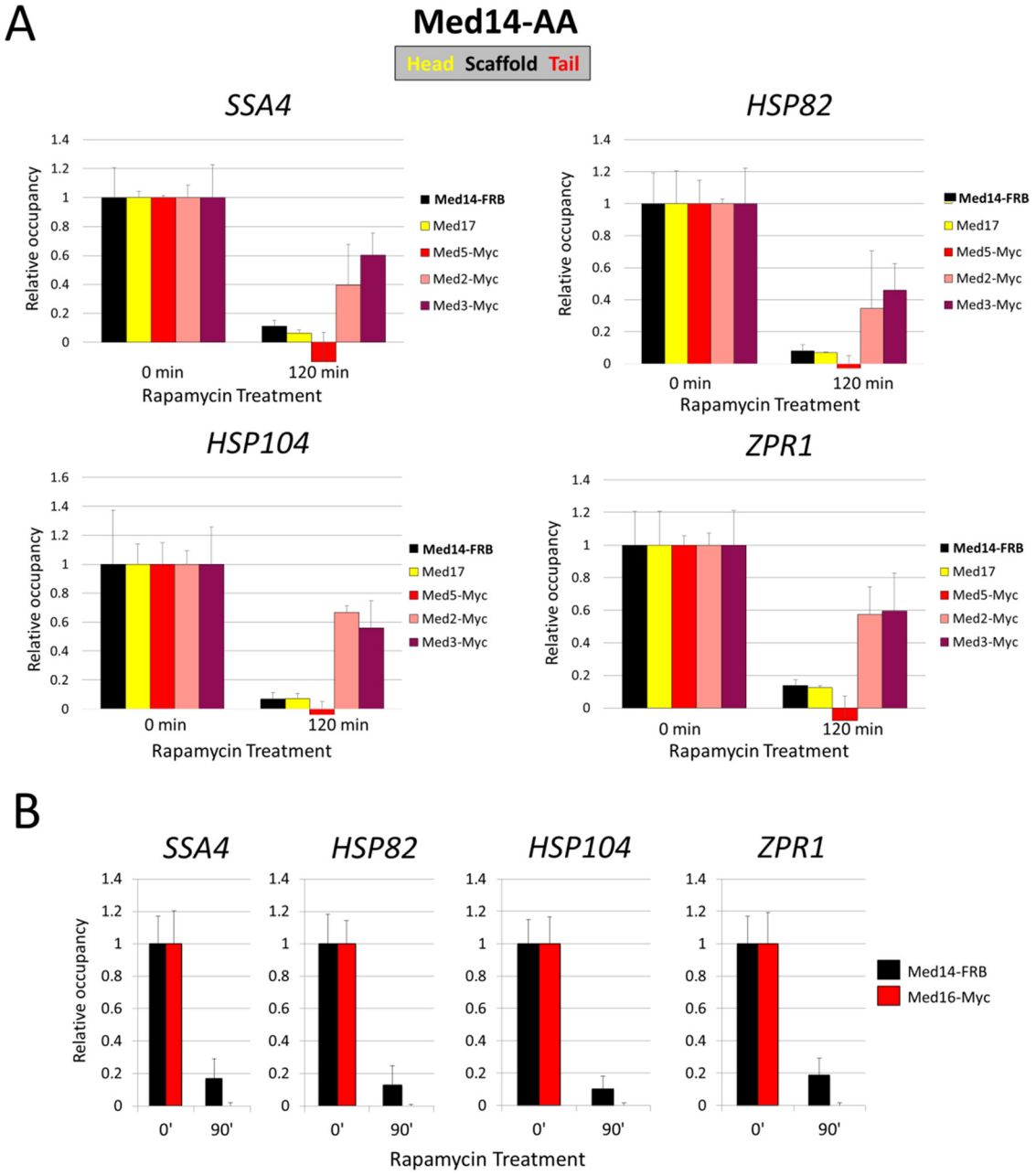


**FIG 3** Cytoplasmic anchoring of scaffold subunit Med14 leads to a strong reduction in Med5 and Med16 occupancy at activated *HSP* genes but only a mild reduction in the occupancy of either Med2 or Med3. (A) ChIP was conducted and quantified as in Fig. 2. Cells were exposed to 1 μg/ml rapamycin for 120 min (or not), followed by a 5-min heat shock. Med14 was detected using anti-FRB Ab; Med17 using anti-Srb4/Med17 antiserum; and Med2, Med3, and Med5 using anti-Myc Ab. Background was determined as described in Fig. 2 and subtracted from each ChIP signal. Means and SD are depicted; $n = 2$ in each case except Med14-FRB ($n = 6$). The strains used were AJ101, AJ102, and AJ103. (B) ChIP analysis was performed and quantified as described for panel A, except that rapamycin pretreatment was for 90 min and Med16 was detected using an anti-Myc Ab. The strain used was YM107.

time course (Fig. 2D and data not shown). Tail subunit Med15 was also depleted in response to rapamycin, yet its depletion, ~40% compared to the untreated control, plateaued 30 min after exposure to drug (Fig. 2D, red bars). CKM subunits Cdk8, Med12, and Med13 likewise were depleted, but here, too, the depletion was less efficient (Fig. 2D, purple, blue, and light-blue bars). The residual occupancy of Med15 and CKM subunits substantially exceeded their occupancy in non-heat-shocked, nondepleted cells (27); thus, what is detected is most likely due to recruitment that takes place upon response to heat shock. Moreover, the depletion observed is unlikely to be due to a nonspecific effect of rapamycin, given that recruitment of Med17, for example, is unaffected by a prior lengthy exposure to rapamycin (see Fig. 7).

We next asked whether the recruitment of other tail subunits persisted in a manner similar to that of Med15. To maximize removal of Med14-FRB from the nucleus, we extended the rapamycin pretreatment to 120 min as part of this analysis. A recent cryo-electron microscopy (cryo-EM) study of purified yeast Me-

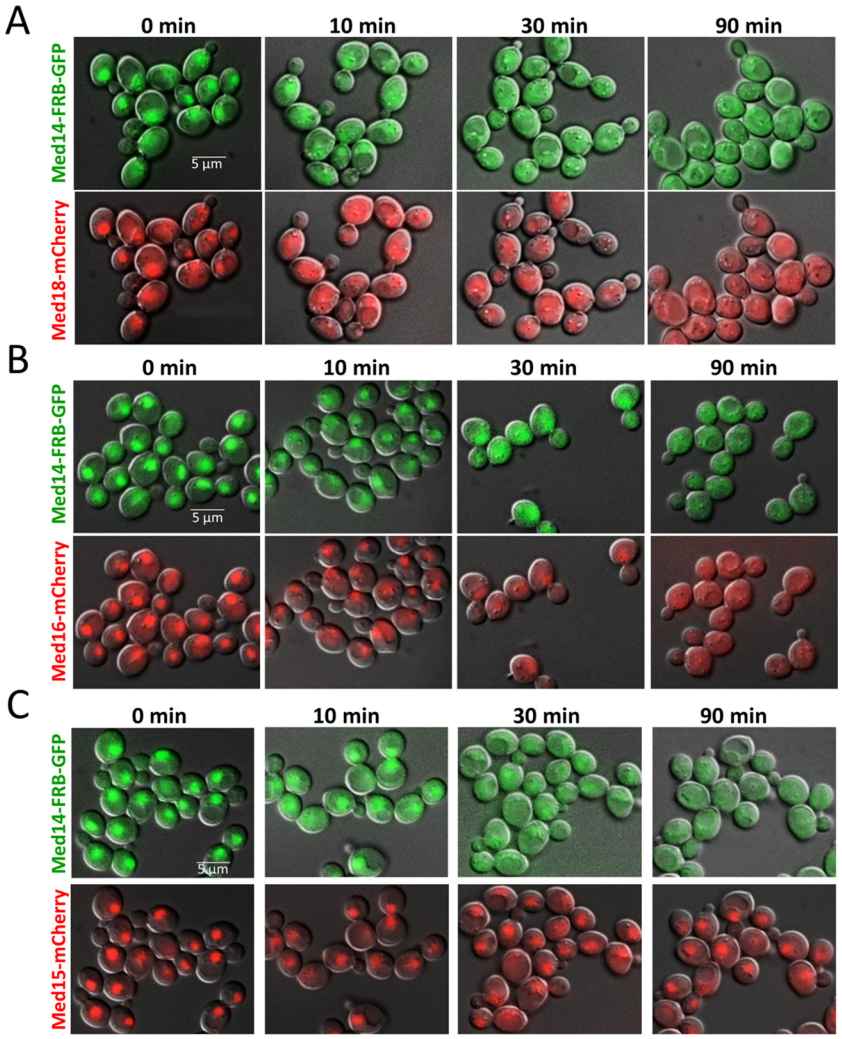


**FIG 4** Med18 and Med16 efficiently relocate from nucleus to cytoplasm following addition of rapamycin to Med14 AA cells, while Med15 persists in the nucleus. Fluorescence microscopy analysis of early-log-phase cells expressing the indicated C-terminally tagged proteins was conducted following addition of rapamycin (1 μg/ml) for the indicated times. The cells were maintained at 25 to 30°C throughout. See Materials and Methods for details. (A) Strain AJ204 (MED14-FRB-GFP, MED18-mCherry). (B) Strain AJ203 (MED14-FRB-GFP, MED16-mCherry). (C) Strain AJ202 (MED14-FRB-GFP, MED15-mCherry).

diator assigned Med15, along with Med2 and Med3, to a central location within the tail in contact with the scaffold subunit Med14, with the Med5-Med16 heterodimer positioned distally (20) (illustrated in Fig. 1A). If this structure were representative of the predominant *in vivo* state, one would predict that the occupancy of the other four tail subunits would resemble Med15 following exposure of Med14 AA cells to rapamycin. However, under these circumstances, only Med2 and Med3 persisted in their recruitment; Med5 and Med16 were depleted to a degree equaling or exceeding that of Med14 (Fig. 3A and B, red bars). Differences in the rates and extents of depletion of subunits suggest the presence of distinct subpopulations of Mediator, certain of which contain Med14-FRB and are cytoplasmically anchored in response to rapamycin, while others lack Med14-FRB and as a consequence remain in the nucleus and are available for recruitment to *HSP* upstream regions.

**Cytoplasmic anchoring of Med14 triggers parallel relocalization of Med18 and Med16 to the cytoplasm, while substantial levels of Med15 remain in the nucleus.** To provide an independent means for assessing the outcome of perturbing Mediator structure via Med14 anchoring, we appended fluorescent tags to the Med14-FRB subunit and representative nonanchored subunits and monitored their subcellular localization by fluorescence microscopy. As shown in Fig. 4, addition of rapamycin to cells cultivated at 30°C led to detectable cytoplasmic localization of Med14-FRB-GFP within 10 min, considerable localization by 30 min, and virtually complete localization by 90 min (Fig. 4A to C). In Med14-FRB-GFP cells expressing either an mCherry-tagged Med18 (head; heterodimeric partner of Med20) or Med16 (tail) subunit, the latter likewise relocated to the cytoplasm with similar kinetics (Fig. 4A and B). This is consistent with ChIP, suggesting a tight linkage between Med14, Med16, and head module subunits. In important contrast, mCherry-tagged tail subunit Med15, expressed in an isogenic Med14-FRB-GFP strain, exhibited different behavior. During the first 10 min, Med15-mCherry relocalized to the cytoplasm to an extent that resembled that of Med14-FRB-GFP (Fig. 4C). However, longer exposures (30 to 90 min) failed to measurably increase cytoplasmic accumulation of this subunit,

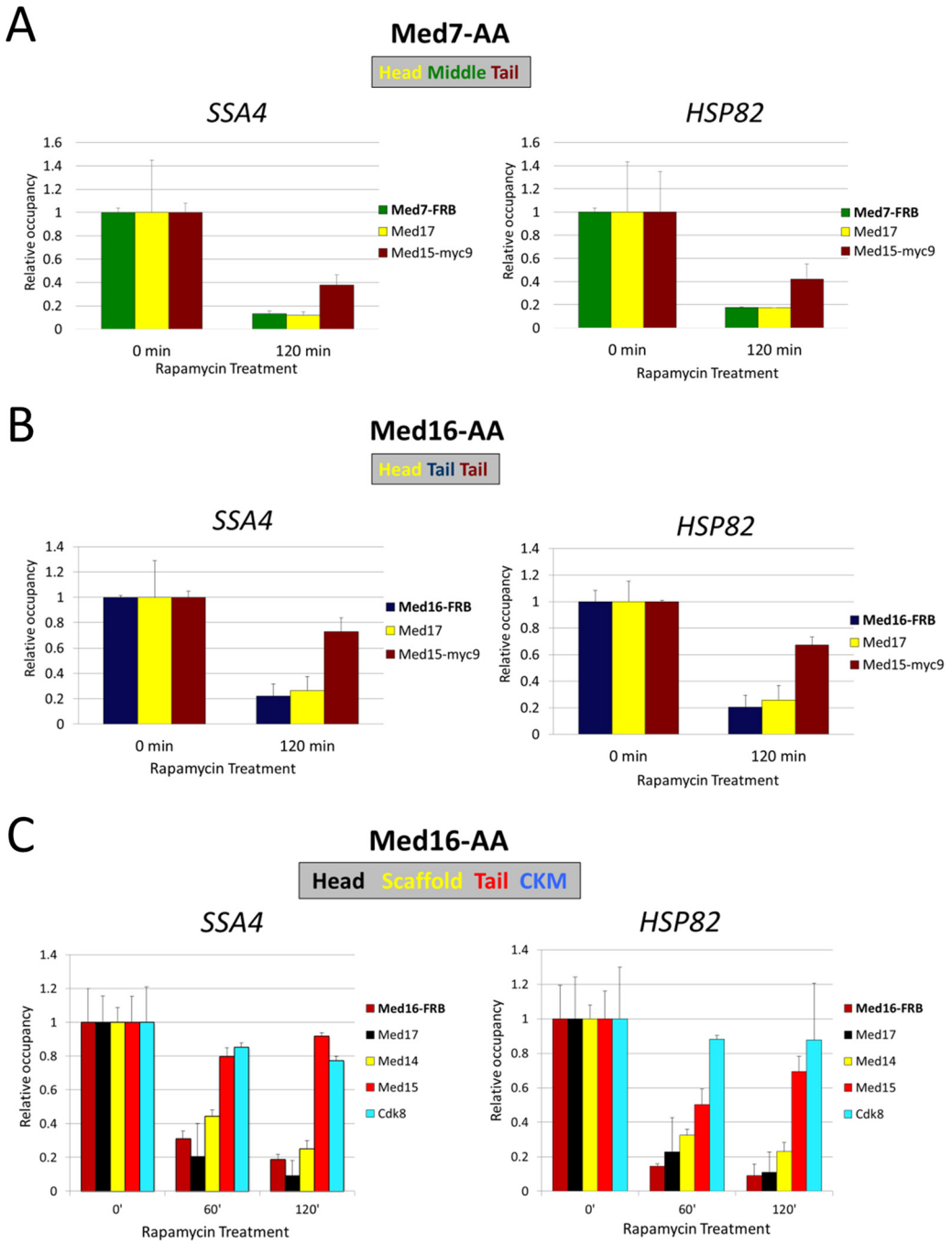


**FIG 5** Anchoring either Med7 or Med16 results in parallel depletion of Med17 but only partial loss of Med15. (A) ChIP analysis of the indicated Mediator subunits was conducted using strain ASK202 and quantified as in Fig. 2. (B) As in panel A, except strain ASK203 was used. For both panels, means and SD are depicted; $n = 2$. (C) As in panel B, except antibodies raised against recombinant proteins were used to detect nontagged proteins; anti-FRB Ab was used to detect Med16. Shown are means and SD; $n = 2$. The strain used was YM124. (B and C) Similar results were obtained with (B) or without (C) C-terminal tagging of Med15.

unlike the anchored protein. Notably, mCherry-tagged Med2 behaved similarly to Med15 (A. S. Kainth and J. Anandhakumar, unpublished observations). Fluorescence microscopy was therefore consistent with ChIP, since both suggest the existence of an independent Med15-containing subcomplex, the Med2-Med3-Med15 triad. ChIP revealed that this complex can be efficiently recruited to *HSP* genes in Med14-anchored cells in response to acute heat shock; fluorescence microscopy indicated that even in non-heat-shocked cells, a substantial fraction of mCherry-tagged Med15 and Med2 remains nuclear when Med14, Med16, and Med18 are largely cytoplasmic. Importantly, a subsequent 5-min heat shock had no effect on the subcellular localization of any of these tagged proteins (A. S. Kainth and J. Anandhakumar, unpublished observations).

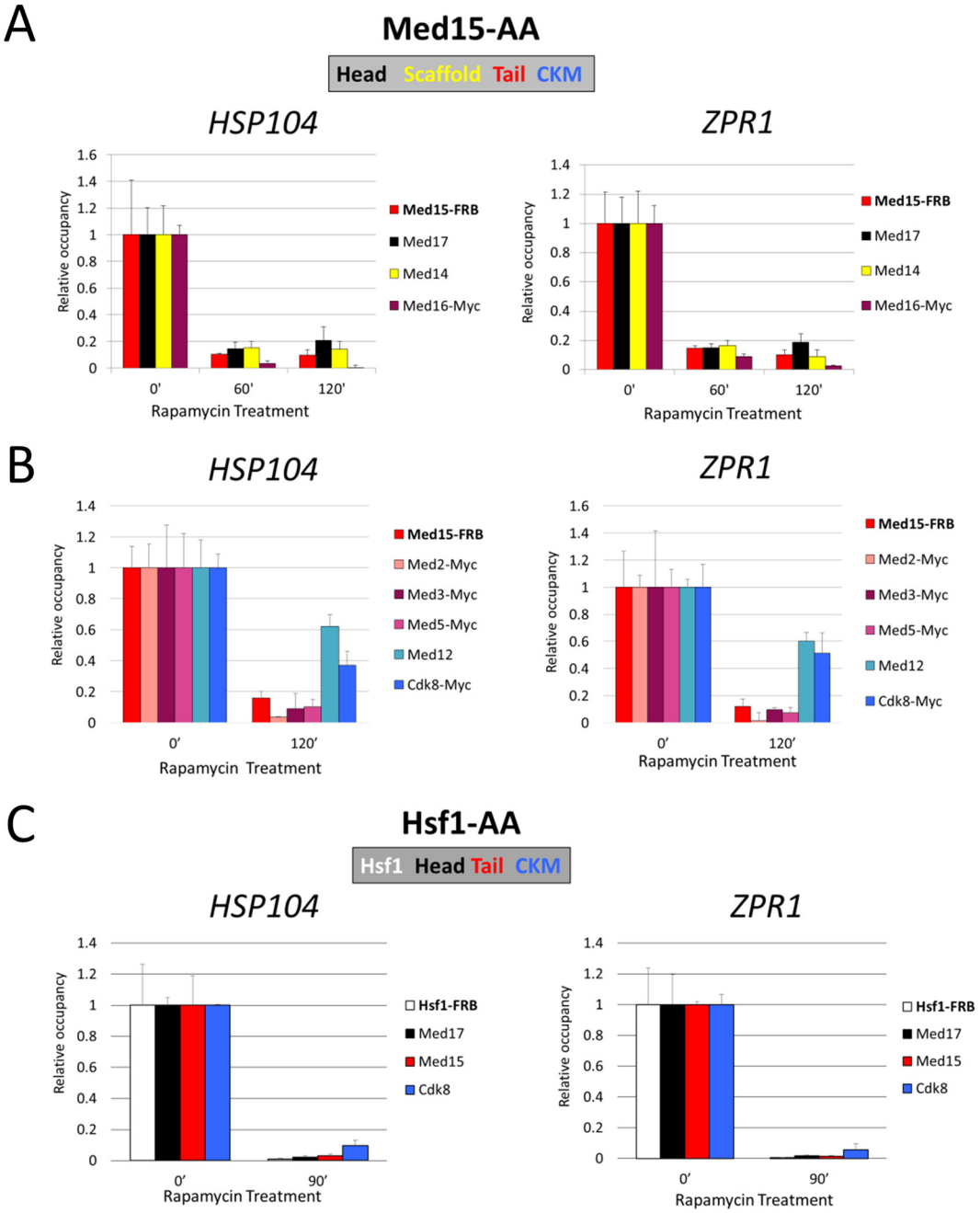


**FIG 6** Anchoring Med15 obviates core Mediator recruitment but not that of the CKM, while anchoring Hsf1 obviates both. (A) ChIP analysis of Med15 AA strain YM125 conducted and quantified as in Fig. 2. Untagged subunits were detected using antibodies raised against the recombinant proteins; Med16-Myc9 was detected using Myc Ab. Means and SD are depicted; $n = 2$ or 3. (B) As in panel A, except Med15 AA strains AJ126, AJ127, AJ128, and YM119 were evaluated. Subunits were detected using antibodies directed against their C-terminal tags; Med12 was detected using anti-Srb8/Med12 antiserum. $n = 2$ for all data except Med15-FRB ($n = 8$). (C) As in panel A, except Hsf1 AA strain BY4742-Hsf1-AA was used. Cells were exposed to rapamycin for 90 min prior to subjecting them to a 5-min heat shock. All proteins were detected using antibodies raised against their recombinant counterparts. $n = 2$ or 3, except in the case of Hsf1 ($n = 5$).

**Anchoring of the middle subunit Med7 depletes head and scaffold subunits while sparing tail subunit Med15.** To address the possibility that the consequences of depleting Med14 represented a special case, we constructed a strain in which the strongly conserved and essential middle module subunit, Med7, was depleted similarly. In addition to its hinge-like function contributing to initiation complex formation discussed above, Med7 impacts *HSP* gene expression through its influence on Pol II elongation (31). Med7-FRB association with acutely induced *HSP* promoters was substantially diminished upon exposure of cells to rapamycin, paralleled by a reduction in both head and scaffold subunits (Fig. 5A and data not shown). Notably, tail subunit Med15 recruitment was less affected. Therefore, depletion of either the scaffold subunit Med14 or middle subunit Med7 leads to the concomitant loss of head and middle subunits, yet

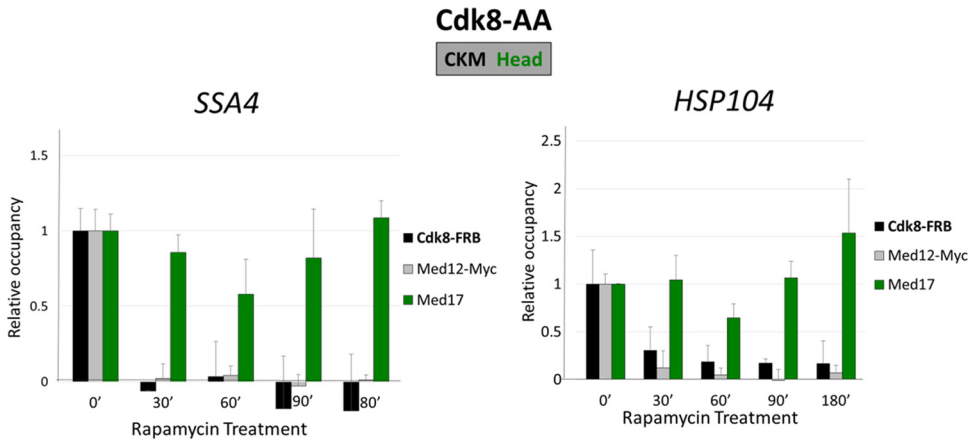


**FIG 7** Anchoring Cdk8 leads to parallel depletion of CKM subunit Med12 but has no effect on Med17 recruitment. ChIP analysis of Cdk8 AA strain YM115. Cells were pretreated with 1 μg/ml rapamycin at 30°C for the times indicated, followed by a 5-min heat shock at 39°C. Depicted are means and SD; $n = 2$. This experiment demonstrates that recruitment of core Mediator (as signified by Med17) to heat shock-induced *HSP* genes is unaffected by prior exposure of cells to rapamycin.

recruitment of tail subunit Med15 (along with Med2 and Med3, where examined) persists.

**Anchoring of tail subunit Med16 depletes most core subunits, yet recruitment of the Med2-Med3-Med15 triad and CKM persists.** We next investigated the effect of depleting tail subunit Med16, given its contrasting behavior (and that of Med5) compared to the other three tail subunits in the Med14-FRB strain. As Med16 and Med5 map distally to the Med2-Med3-Med15 triad, their principal physical connection to the rest of Mediator based on a current model (20), it might be anticipated that anchoring Med16 would result in a corresponding depletion of Med5 and possibly also of the triad. In addition, secondary to loss of Med15, recruitment of the rest of Mediator should be severely reduced, given that Med15 is the principal physical and/or functional target of Hsf1 (27). However, in contrast to this expectation, Med15 recruitment was only mildly affected by Med16 depletion (reduced ~20 to 30%), while both Med14 and Med17 were severely affected (Fig. 5B and C). Also notable, and in contrast to prevailing models, Cdk8 recruitment was relatively unaffected by anchoring of Med16 despite the apparent loss of both the head and middle modules.

**Anchoring of tail subunit Med15 depletes all tested core subunits, yet recruitment of the CKM persists.** We next addressed the consequences of depleting Med15 itself. If Hsf1 recruits Mediator principally through its interaction with Med15, then Med15 depletion should severely diminish recruitment of head, middle, tail, and kinase subunits. Consistent with this prediction, efficient (80 to 90%) depletion of Med15 typically resulted in an equally severe reduction in other core subunits, including Med17, Med14, and all four tail subunits (Fig. 6A and B). Nonetheless, a substantial fraction (~50%) of the Cdk8-kinase module was recruited to *HSP* genes in the absence of the core complex (Fig. 6B). To ascertain whether Hsf1 itself was required for CKM recruitment, we conditionally depleted it. As demonstrated by fluorescence microscopy, GFP-tagged Hsf1-FRB molecules were efficiently depleted from the nucleus upon exposure of cells to rapamycin for 30 to 45 min (data not shown). Following Hsf1 depletion, neither core subunits Med15 and Med17 nor CKM subunit Cdk8 could be detected in heat shock-induced *HSP* UAS regions (Fig. 6C). Therefore, while the CKM can be recruited to *HSP* genes independently of core Mediator in response to heat shock, its recruitment is dependent on Hsf1.

**Anchoring of the CKM has no effect on core mediator recruitment.** To investigate whether the CKM contributes to core Mediator recruitment, we conditionally anchored Cdk8. As shown in Fig. 7, Cdk8-FRB was prevented from binding *HSP* UAS/promoter regions in cells pretreated with rapamycin for as little as 30 min. Paralleling the loss of Cdk8 occupancy was loss of Med12, suggesting that the CKM itself was efficiently depleted from the nucleus. In contrast, Med17 occupancy was not affected, even in cells pretreated with rapamycin for as long as 180 min, arguing that the CKM plays little or no role in recruitment of core Mediator to these genes.

**Med14 anchoring affects Pol II recruitment, Pol II elongation, nucleosome displacement, and mRNA synthesis.** Given the central role that Mediator plays in Pol II transcription, we hypothesized that its disruption would severely impact *HSP* gene activation. Indeed, Pol II occupancy within acutely activated *HSP* promoter regions was progressively reduced in parallel with Med17 in Med14 AA cells exposed to rapamycin (Fig. 8A). Interestingly, despite a strong reduction in Pol II promoter abundance—which may reflect reduced recruitment, reduced dwell time (an increased rate of Pol II promoter escape), or a combination of the two—Pol II occupancy within *HSP* coding regions was less affected (Fig. 8B). Nonetheless, transcription was strongly reduced in rapamycin-treated cells subjected to either 2.5 or 15 min of heat shock, as assayed by RT-qPCR (Fig. 8C). Consistent with reduced transcription, nucleosomal eviction within *HSP* gene coding regions was diminished (65). Taken together, these observations are consistent with a role for Mediator in regulating not only Pol II recruitment, but also one or more postrecruitment steps, including polymerase elongation rate/processivity and nucleosome disassembly, in accord with previous genetic analysis (31). The residual expression seen in rapamycin-treated cells could reflect the small amount of holo-Mediator recruitment that persists under these conditions (5 to 10%) (Fig. 2D), the contribution of the Med2-Med3-Med15 triad, and/or contributions of other transcriptional coactivators (see below).

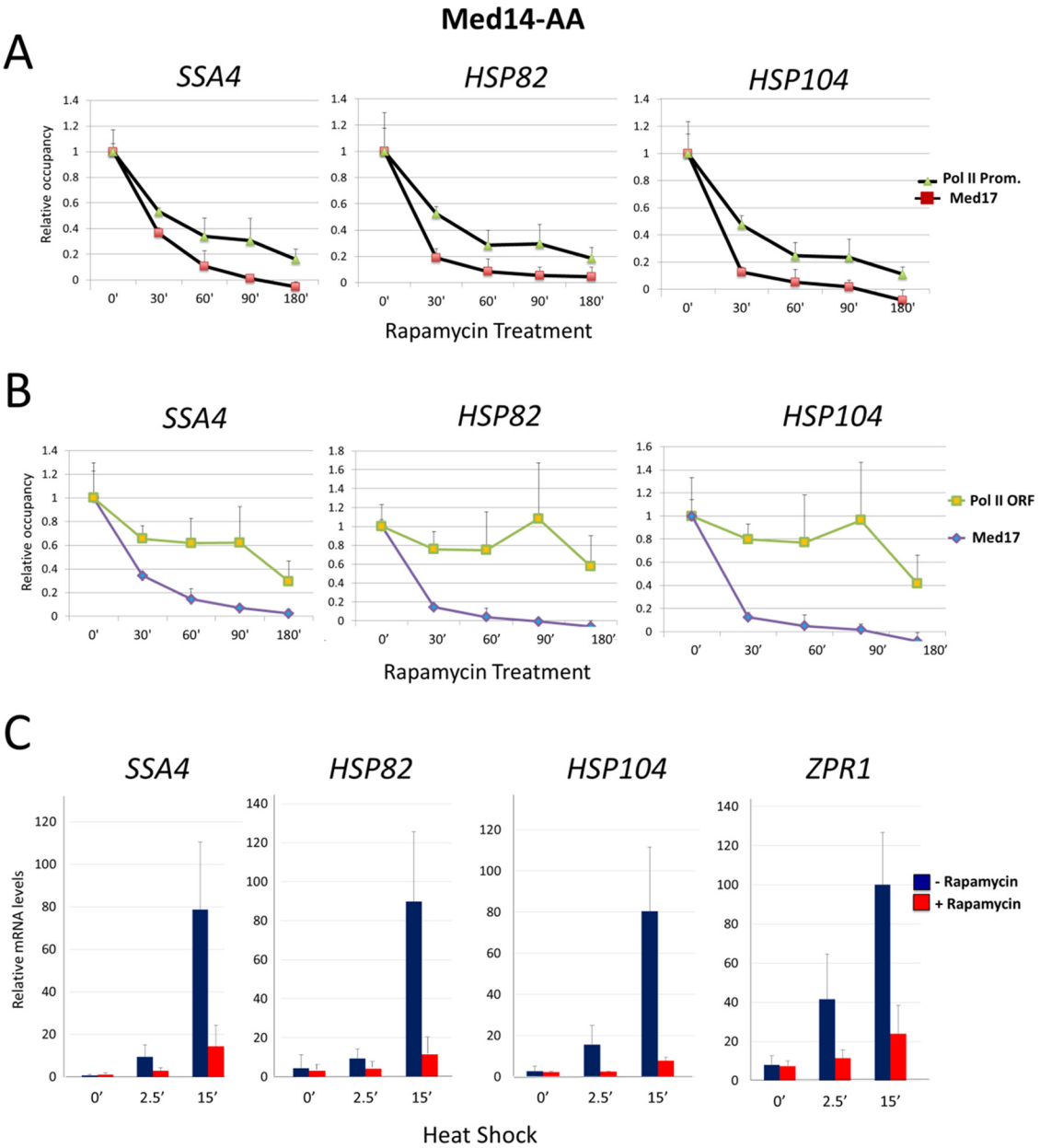


**FIG 8** Anchoring Med14 strongly reduces Pol II promoter occupancy and *HSP* gene expression during heat shock. (A) Pol II and Med17 ChIP analysis of strain YM103 pretreated with rapamycin for the indicated times, followed by 5-min heat shock. Depicted is Pol II occupancy at *HSP* gene promoters and Med17 occupancy at *HSP* UAS regions. Shown are means and SD; $n = 3$ or 4. (B) Same as panel A, except Pol II occupancy within *HSP* coding regions is shown. (C) RT-qPCR analysis of *HSP* mRNA levels in YM103 cells either pretreated or not with rapamycin for 90 min (red and blue bars, respectively), followed by heat shock for the indicated times. Shown are means and SD; $n \geq 2$.

**Anchoring of Med15 affects *HSP* gene expression equivalently to anchoring of either Med14 or Med16, while anchoring of Cdk8 has no effect.** We next examined the impact of anchoring the tail subunits Med15 and Med16 on *HSP* gene transcription and examined additional time points of expression. If the severity of Mediator's structural perturbation is functionally correlated with *HSP* gene expression, then depletion of Med16 should affect *HSP* transcription to approximately the same degree as Med14 depletion despite their different locations and functional roles within the core complex. On the other hand, depletion of Med15, which nearly obviated recruitment of core Mediator, might be expected to have a more severe effect. However, RT-qPCR analysis revealed that disruption of Mediator via anchoring of either Med16 or Med15 had a very similar effect on expression: severe reduction (5- to 10-fold) in *HSP* transcript accumulation for the first 45 min of heat shock (Fig. 9A and B). This phenotype closely resembles that of the Med14 AA strain (Fig. 8C) and, moreover, indicates that recruitment of the tail triad does not detectably affect *HSP* gene expression. Depletion of the CKM through anchoring of the Cdk8 subunit had little or no effect on *HSP* gene expression throughout a 180-min heat shock time course (Fig. 9C), consistent with the absence of an effect on core Mediator recruitment (Fig. 7).

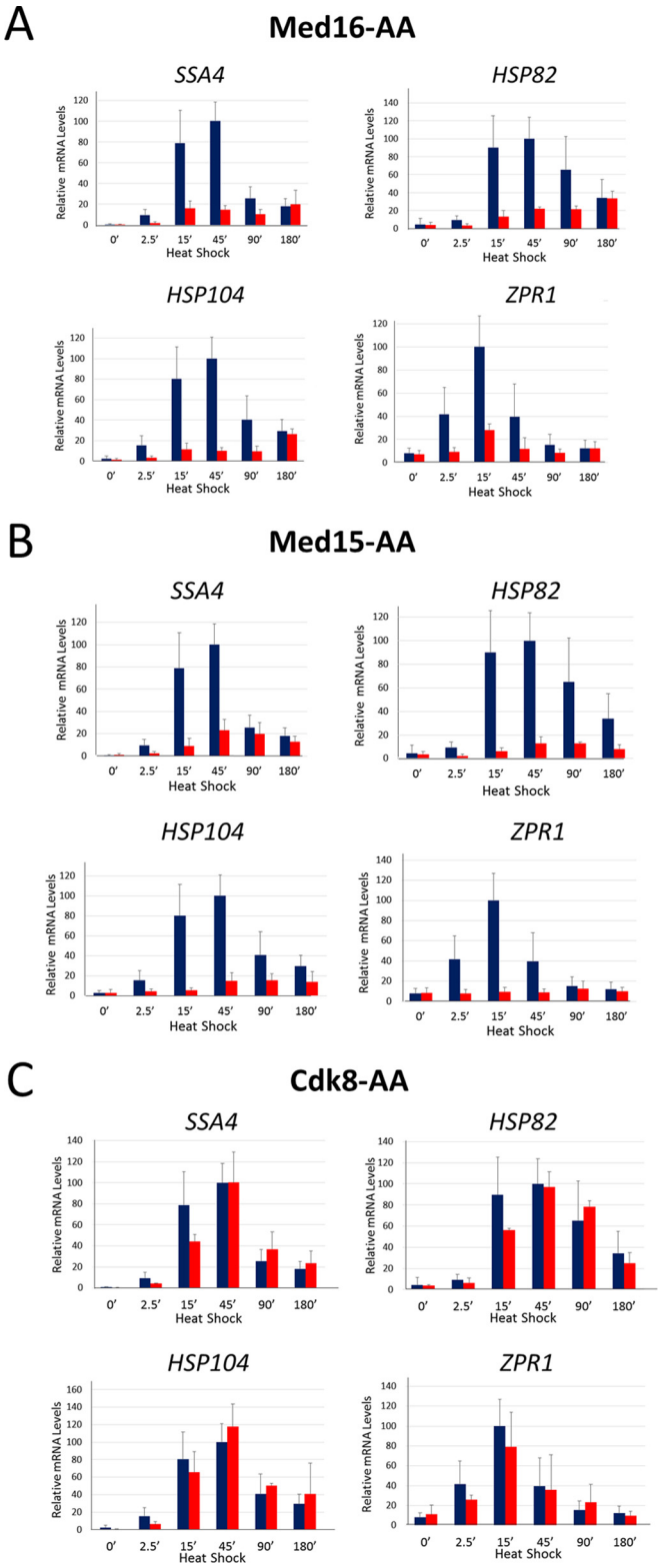


**FIG 9** Anchoring of either tail subunit, Med15 or Med16, strongly reduces *HSP* gene transcription whereas anchoring of Cdk8 has no effect. (A) RT-qPCR analysis of Med16-FRB strain YM124 subjected to a heat shock time course following pretreatment or not with rapamycin as in Fig. 8C. Shown are means and SD; $n \geq 2$. Blue bars, without rapamycin; red bars, with rapamycin. (B) As for panel A, except Med15-FRB strain YM117 was analyzed. (C) As for panel A, except Cdk8-FRB strain YM115 was analyzed.

**Mediator recruitment to HSP genes occurs independently of SAGA.** The results of the above-described experiments, together with an earlier ChIP analysis of Mediator and Hsf1 activation domain mutants (27), argue that Mediator recruitment to *HSP* genes occurs principally through physical interaction between Hsf1 activation domains and the tail module subunit Med15. However, as analysis of other activators has suggested a complex relationship between Mediator and the conserved and essential SAGA coactivator, we wished to take advantage of the anchor away technique to ask whether Mediator recruitment is facilitated by SAGA, as has been claimed for Gal4-regulated genes (66), or whether Mediator recruitment occurs independently of SAGA, as is the case for other activators, including Swi5, Gcn4, and Met4 (9, 67, 68).

As shown in Fig. 10A, conditional inactivation of SAGA—achieved through anchoring of the essential core subunit Spt20—did not impair the recruitment of head subunit Med17 or either of two CKM subunits, Cdk8 and Med12, to *HSP* genes. In fact, recruitment of Med17 may have been enhanced, at least in one case (Fig. 10A, asterisk). This indicates that the recruitment of both core Mediator and CKM occurs independently of SAGA. Finally, we asked the reciprocal question, namely, whether SAGA recruitment is affected by prior Mediator depletion. In Med14-anchored cells, SAGA occupancy (as signified by its Spt3 subunit) was unaffected at two *HSP* genes, although it was reduced ~2-fold at two others (Fig. 10B). These results suggest that SAGA recruitment may be facilitated by Mediator, at least in certain contexts.

## DISCUSSION

**Evidence for multiple mediator subcomplexes in yeast.** Current models typically portray yeast core Mediator as a monolithic, tri-modular complex (16, 20, 21, 49, 69) (Fig. 1A). In this regard, the yeast core complex appears to differ from that of metazoan Mediator, which while also trimodular, has been suggested to exist in multiple species (reviewed in references 4, 5, and 7). In contrast to this monolithic view, we provide evidence that yeast Mediator likewise exists in multiple species *in vivo*.

ChIP assays revealed that recruitment of three tail subunits—Med2, Med3, and Med15—to activated *HSP* UAS/promoter regions persists under circumstances under which other core subunits fail to be detected. Under these circumstances, brought about by conditional cytoplasmic anchoring of Med7, Med14, or Med16, approximately 50% of Med15 (as well as Med2 and Med3, where tested) continue to be recruited. This suggests the existence of two Med15-containing complexes in anchor away strains, one of which remains nuclear and is recruited to *HSP* genes while the other is cytoplasmically anchored in parallel with the FRB-tagged subunit and thus is unavailable for recruitment. Subcellular localization analysis supports this view, as head subunit Med18 and tail subunit Med16 are rapidly depleted from the nucleus in a Med14 AA strain exposed to rapamycin, closely resembling the kinetics with which Med14 itself is depleted. In contrast, Med15 is only partially relocalized to the cytoplasm, although the relocalization that does occur is rapid. Thus, both ChIP and fluorescence microscopy are consistent with the idea that Med15 is present in two complexes: the intact, 21-subunit core complex and the Med2-Med3-Med15 triad. Moreover, a third complex, comprised of the normal head and middle subunits, as well as scaffold subunit Med14 and two tail subunits (Med5 and Med16), also likely exists (schematically summarized in Fig. 11).

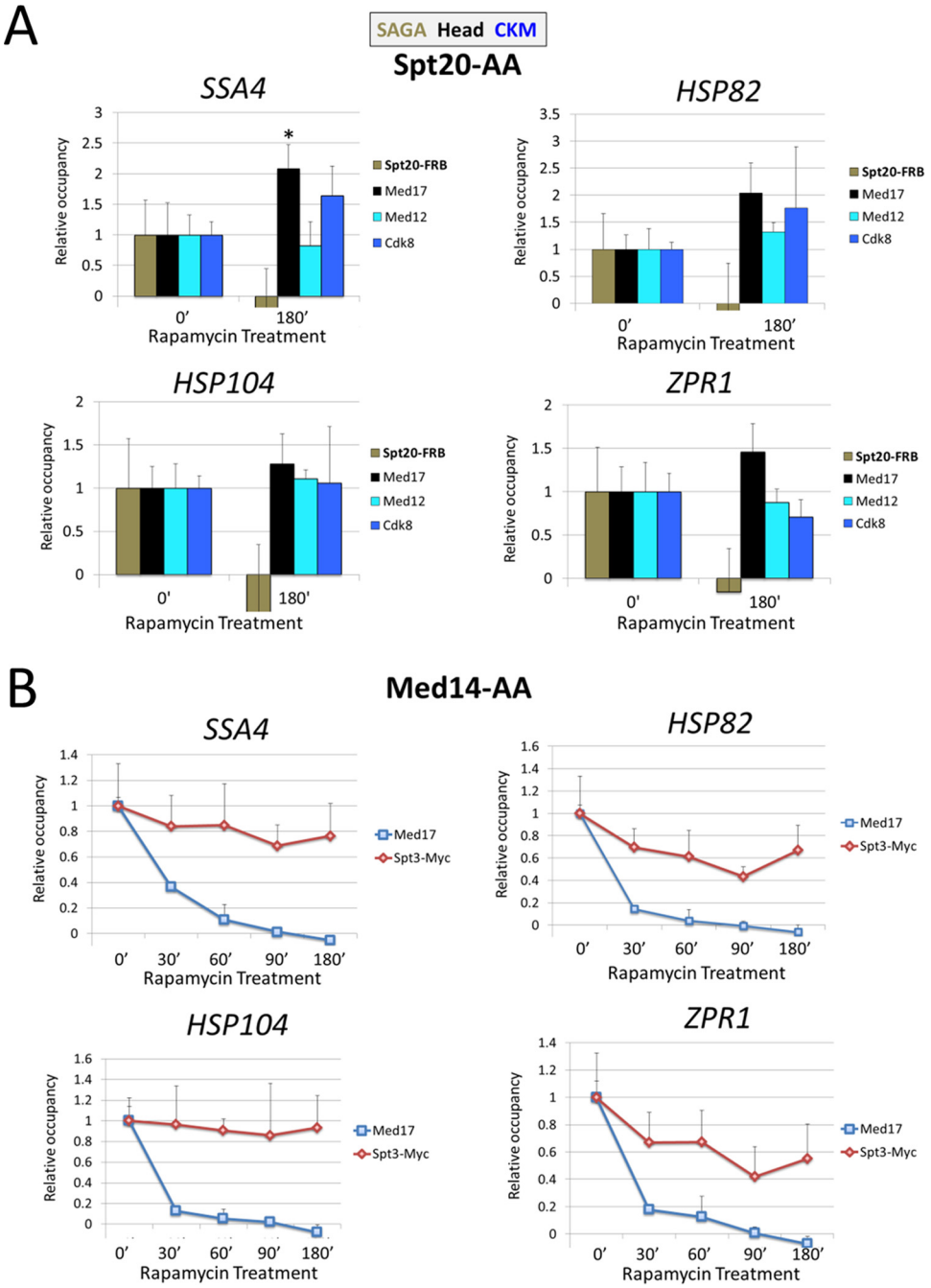


**FIG 10** Nuclear depletion of SAGA subunit Spt20 has minimal effect on CKM-Mediator recruitment to heat shock-induced *HSP* genes. (A) ChIP analysis of SAGA subunit Spt20-FRB, core Mediator subunit Med17, and CKM subunits Med12 and Cdk8 in strain YM120 exposed to rapamycin for the indicated times, followed by a 5-min heat shock. Shown are means and SD; $n = 3$. The asterisk indicates that occupancy significantly differs from that of the control (0′) condition ($P < 0.05$; two-tailed *t* test; equal variance). (B) As in panel A, except Med14-FRB strain YM108 was analyzed, and occupancy of Med17 and SAGA subunit Spt3 was evaluated.

Our data are therefore consistent with the idea that the 21-subunit core complex exists in dynamic equilibrium with the 18-subunit and 3-subunit subcomplexes and that anchoring of Med7, Med14, or Med16 uncovers the existence of subcomplexes that exist in equilibrium with the intact core under normal conditions. An important assumption underlying our model is equal stoichiometry of the triad with other core subunits. Such an assumption appears to be warranted, in that a recent single-cell proteomic analysis revealed that most core subunits are present in similar numbers (~75 to 150 molecules) in wild-type haploid cells (70). A second assumption is that the anchor away technique *per se* does not trigger dissociation of labile subunits from core Mediator. While we cannot fully rule this out, it is notable that, as mentioned above, essentially identical results were obtained irrespective of whether a scaffold (Med14), middle (Med7), or tail (Med16) subunit was anchored. In all three cases, the Med2-Med3-Med15

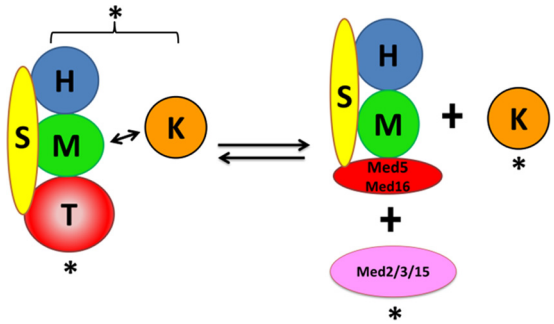


**FIG 11** Yeast Mediator complexes suggested by this study. Evidence obtained from both ChIP and fluorescence microscopy analyses of AA strains suggests the existence of multiple Mediator complexes *in vivo*. Those marked with asterisks were detected at the regulatory regions of heat shock-induced *HSP* genes. Note that the relative abundances of the Mediator species depicted may differ in wild-type strains versus the AA strains examined here. In particular, dissociation of intact core Mediator into tail triad and 18-mer subcomplexes, suggested by the ChIP data (Fig. 2, 3, 5, and 6), may be more pronounced in AA strains. H, head; M, middle; T, tail; S, scaffold; K, kinase.

triad continued to be recruited to *HSP* genes while the remainder of the core complex was not.

Moreover, our results are in accord with previous observations by Liu and colleagues that two principal forms of Mediator can be isolated from yeast nuclear extracts using an epitope-tagging strategy (71). One complex isolated by these authors corresponded to intact 24-subunit CKM-Mediator, while the other, dubbed "Mediator core" (Medc), contained most head and middle subunits but lacked the tail and CKM. By several criteria, Medc was not derived from dissociation of intact Mediator, but rather represented a preexisting complex (71). Medc therefore resembles the 18-subunit subassembly lacking the tail triad that we hypothesize is codepleted along with intact core Mediator in Med7, Med14, and Med16 AA strains.

A number of studies of yeast mutants, including the *sin4*Δ (*med16*Δ), *rgr1*-Δ*2* (*med14*-Δ*2*), and *med17 ts* mutants, have likewise reported evidence for the existence of independent subcomplexes using a variety of assays, including ChIP (50), ChIP sequencing (ChIP-seq) (61), biochemical purification (51), and cryo-EM (49). However, since these studies used conventional mutants, it is difficult to rule out the possibility that the chronic presence of a mutant form of Mediator confounded the outcome. Thus, for example, the existence of the tail triad, as originally observed by Zhang and coworkers, could not be assumed to represent the normal physiological state, since their biochemical and ChIP analyses were done in a *sin4*Δ mutant (50). The AA approach described here, in which cells experience minimal genetic perturbation until the addition of rapamycin, grow normally at 30°C in the absence of the drug (see Fig. S1 in the supplemental material), and retain full viability even when pretreated for 120 min with rapamycin (see Fig. S2 in the supplemental material), represents an important step toward circumventing this problem.

In addition, we suggest that our observations inform recent detailed architectural analyses of purified core Mediator complexes isolated from *S. cerevisiae*. Using an electron microscopy labeling strategy to identify the locations of tail module subunits, Tsai and colleagues placed the triad in the middle of the tail and the Med5-Med16 heterodimer distal (20). Likewise, Robinson and colleagues, using a combination of chemical cross-linking, X-ray crystallography, homology modeling, and cryo-EM electron density mapping, similarly placed the triad in a central location within the tail, although in their model, both Med15 and Med16 made contact with the scaffold subunit Med14 (21). Our data suggest that the Med2-Med3-Med15 triad is less stably associated with Med14 and the rest of the essential core complex than is Med16 and in fact likely preexists as an independent subpopulation. Underscoring this idea is the striking difference in subcellular localizations of Med15-mCherry and Med16-mCherry in isogenic Med14 AA strains briefly exposed to rapamycin. Moreover, Robinson and colleagues suggested that Med15 stabilizes the interaction of Med16, as well as that of Med5, with the tail (21). While this may be true, it is interesting that Med16 depletion did not lead to a parallel loss of Med15. Our observations are consistent with Med2-Med3-Med15 and Med5-Med16 constituting structurally and functionally independent subcomplexes within the tail.

**Hsf1 Recruits the CKM to its target genes independently of core Mediator.** A novel finding of this study is that in addition to its recruitment as part of holo-Mediator, the CKM can be recruited independently of the core complex. This is in contrast with current models which suggest that in both yeast and humans, CKM recruitment to regulatory DNA sequences occurs as a consequence of its interaction with core Mediator that is itself the physical target of a gene-specific transcription factor (20, 64; reviewed in reference 5). This observation therefore raises the possibility that multiple mechanisms exist to ensure CKM recruitment to activated *HSP* genes. In light of this, it is puzzling that a functional role for the CKM in *HSP* gene regulation has proven elusive. As shown here, neither mRNA accumulation nor core Mediator recruitment was affected upon CKM depletion. It is possible that the CKM plays a more subtle role, such as fine-tuning the rapid induction kinetics (best unveiled using instantaneous transcription measurements) or in regulating one or more posttranscriptional steps in *HSP* gene expression, questions beyond the scope of the current study. A provocative implication of this and the above-mentioned findings is that in certain contexts, individual modules can be recruited by gene-specific transcription factors independently of the rest of Mediator. If this also applies to human cells, it may provide an explanation for the oncogene-specific effect of somatic mutations in CKM subunits Med12L and Med13 (reviewed in reference 7).

**Hsf1 targets the tail triad in its SAGA-independent recruitment of Mediator.** Our AA experiments support earlier conclusions, derived from detailed ChIP analyses of deletion mutants (*med15*Δ, *med16*Δ, and *med15*Δ *med16*Δ mutants), that Hsf1 interacts directly or indirectly with Med15 (27). Indeed, as discussed above, we demonstrate the persistent recruitment of the Med2-Med3-Med15 triad in circumstances under which recruitment of all other head, middle/scaffold, and tail subunits examined was severely reduced or eliminated. Importantly, our experiments do not rule out the possibility that Hsf1 targets additional subunits within core Mediator, including Med16 as previously suggested (27). Reduced recruitment of Med15 in cells conditionally depleted of Med16 is consistent with Med16 serving as a secondary target of Hsf1. In addition, we provide evidence that CKM-Mediator recruitment to *HSP* genes is unimpeded in cells depleted of the essential SAGA subunit Spt20. This implies that Hsf1's recruitment of Mediator occurs independently of SAGA and that Hsf1 is

similar in this regard to a number of other yeast TFs that independently target Mediator and SAGA in their regulation of Pol II transcription (8–10, 67, 68).

**Mediator regulates postrecruitment steps at *HSP* genes.** Use of the powerful AA technique provides support for a previous suggestion that Mediator, in particular its middle module, participates in regulating Pol II postrecruitment steps, including promoter escape, elongation rate, and processivity (31). This conclusion arises from the observation that in a Med14 cytoplasmically anchored strain, Pol II abundance within *HSP* coding regions is only modestly affected despite an ~80% reduction in mRNA accumulation. Concomitantly, we observed that nucleosome eviction over these coding regions is substantially reduced (65). While not addressed here, anchoring of Med14-containing Mediator complexes could affect Pol II elongation by depleting elongation factors that normally associate with Mediator at the promoter. Whatever the underlying mechanism, these results closely resemble previous observations of several middle module mutants isolated in a genetic screen for regulators of *HSP* transcription (31). Together, they argue for an expanded role for Mediator in regulating *HSP* gene transcription beyond recruitment and assembly of the transcription initiation complex.

## ACKNOWLEDGMENTS

We thank Kelly Tatchell for facilities, reagents, assistance with fluorescence microscopy, and helpful discussions; Denes Hnisz and Sunyoung Kim for critical reading of the manuscript; Richard Young, Steve Hahn, Mark Ptashne, and David Stillman for antibodies; Frank Holstege for yeast strains; and David Pincus and Kim Nasmyth for plasmids.

Y.W.M. and D.S.G. conceived the study. Y.W.M., A.S.K., J.A., S.C., and D.S.G. designed the experiments. J.A., Y.W.M., S.C., and A.S.K. performed the experiments. Y.W.M., J.A., A.S.K., S.C., and D.S.G. interpreted the data. D.S.G. wrote the paper.

## FUNDING INFORMATION

This work, including the efforts of David S. Gross, was funded by National Science Foundation (NSF) (MCB-1025025 and MCB-1518345). This work, including the efforts of Jayamani Anandhakumar, was funded by Feist-Weiller Cancer Center (FWCC Postdoctoral Fellowship). This work, including the efforts of Yara W. Moustafa, was funded by LSUHSC Research Foundation (Ike Muslow Predoctoral Fellowship).

The funders of this study had no role in study design, data collection and interpretation, or the decision to submit the work for publication.

## REFERENCES

1. **Whyte WA, Orlando DA, Hnisz D, Abraham BJ, Lin CY, Kagey MH, Rahl PB, Lee TI, Young RA.** 2013. Master transcription factors and Mediator establish super-enhancers at key cell identity genes. Cell **153:** 307–319. http://dx.doi.org/10.1016/j.cell.2013.03.035.
2. **Haber JE.** 2012. Mating-type genes and MAT switching in Saccharomyces cerevisiae. Genetics **191:**33–64. http://dx.doi.org/10.1534/genetics.111.134577.
3. **Hnisz D, Abraham BJ, Lee TI, Lau A, Saint-Andre V, Sigova AA, Hoke HA, Young RA.** 2013. Super-enhancers in the control of cell identity and disease. Cell **155:**934–947. http://dx.doi.org/10.1016/j.cell.2013.09.053.
4. **Malik S, Roeder RG.** 2010. The metazoan Mediator co-activator complex as an integrative hub for transcriptional regulation. Nat Rev Genet **11:** 761–772. http://dx.doi.org/10.1038/nrg2901.
5. **Poss ZC, Ebmeier CC, Taatjes DJ.** 2013. The Mediator complex and transcription regulation. Crit Rev Biochem Mol Biol **48:**575–608. http://dx.doi.org/10.3109/10409238.2013.840259.
6. **Ansari SA, Morse RH.** 2013. Mechanisms of Mediator complex action in transcriptional activation. Cell Mol Life Sci **70:**2743–2756. http://dx.doi.org/10.1007/s00018-013-1265-9.
7. **Allen BL, Taatjes DJ.** 2015. The Mediator complex: a central integrator of transcription. Nat Rev Mol Cell Biol **16:**155–166. http://dx.doi.org/10.1038/nrm3951.
8. **Bryant GO, Ptashne M.** 2003. Independent recruitment in vivo by Gal4 of two complexes required for transcription. Mol Cell **11:**1301–1309. http://dx.doi.org/10.1016/S1097-2765(03)00144-8.
9. **Fishburn J, Mohibullah N, Hahn S.** 2005. Function of a eukaryotic transcription activator during the transcription cycle. Mol Cell **18:**369–378. http://dx.doi.org/10.1016/j.molcel.2005.03.029.
10. **Reeves WM, Hahn S.** 2005. Targets of the Gal4 transcription activator in functional transcription complexes. Mol Cell Biol **25:**9092–9102. http://dx.doi.org/10.1128/MCB.25.20.9092-9102.2005.
11. **Yang F, Vought BW, Satterlee JS, Walker AK, Jim Sun ZY, Watts JL, DeBeaumont R, Saito RM, Hyberts SG, Yang S, Macol C, Iyer L, Tjian R, van den Heuvel S, Hart AC, Wagner G, Naar AM.** 2006. An ARC/Mediator subunit required for SREBP control of cholesterol and lipid homeostasis. Nature **442:**700–704. http://dx.doi.org/10.1038/nature04942.
12. **Spaeth JM, Kim NH, Boyer TG.** 2011. Mediator and human disease. Semin Cell Dev Biol **22:**776–787. http://dx.doi.org/10.1016/j.semcdb.2011.07.024.
13. **Lariviere L, Plaschka C, Seizl M, Wenzeck L, Kurth F, Cramer P.** 2012. Structure of the Mediator head module. Nature **492:**448–451. http://dx.doi.org/10.1038/nature11670.
14. **Esnault C, Ghavi-Helm Y, Brun S, Soutourina J, Van Berkum N, Boschiero C, Holstege F, Werner M.** 2008. Mediator-dependent recruitment of TFIIH modules in preinitiation complex. Mol Cell **31:**337–346. http://dx.doi.org/10.1016/j.molcel.2008.06.021.
15. **Soutourina J, Wydau S, Ambroise Y, Boschiero C, Werner M.** 2011. Direct interaction of RNA polymerase II and Mediator required for transcription in vivo. Science **331:**1451–1454. http://dx.doi.org/10.1126/science.1200188.
16. **Plaschka C, Lariviere L, Wenzeck L, Seizl M, Hemann M, Tegunov D, Petrotchenko EV, Borchers CH, Baumeister W, Herzog F, Villa E, Cramer P.** 2015. Architecture of the RNA polymerase II-Mediator core initiation complex. Nature **518:**376–380. http://dx.doi.org/10.1038/nature14229.
17. **Robinson PJ, Bushnell DA, Trnka MJ, Burlingame AL, Kornberg RD.** 2012. Structure of the Mediator head module bound to the carboxy-terminal domain of RNA polymerase II. Proc Natl Acad Sci U S A **109:** 17931–17935. http://dx.doi.org/10.1073/pnas.1215241109.
18. **Cai G, Imasaki T, Yamada K, Cardelli F, Takagi Y, Asturias FJ.** 2010. Mediator head module structure and functional interactions. Nat Struct Mol Biol **17:**273–279. http://dx.doi.org/10.1038/nsmb.1757.
19. **Cevher MA, Shi Y, Li D, Chait BT, Malik S, Roeder RG.** 2014. Reconstitution of active human core Mediator complex reveals a critical role of the MED14 subunit. Nat Struct Mol Biol **21:**1028–1034. http://dx.doi.org/10.1038/nsmb.2914.
20. **Tsai KL, Tomomori-Sato C, Sato S, Conaway RC, Conaway JW, Asturias FJ.** 2014. Subunit architecture and functional modular rearrangements of the transcriptional Mediator complex. Cell **157:**1430–1444. http://dx.doi.org/10.1016/j.cell.2014.05.015.
21. **Robinson PJ, Trnka MJ, Pellarin R, Greenberg CH, Bushnell DA, Davis R, Burlingame AL, Sali A, Kornberg RD.** 2015. Molecular architecture of the yeast Mediator complex. eLife **4:**e08719. http://dx.doi.org/10.7554/eLife.08719.
22. **Baumli S, Hoeppner S, Cramer P.** 2005. A conserved mediator hinge revealed in the structure of the MED7.MED21 (Med7.Srb7) heterodimer. J Biol Chem **280:**18171–18178. http://dx.doi.org/10.1074/jbc.M413466200.
23. **Herbig E, Warfield L, Fish L, Fishburn J, Knutson BA, Moorefield B, Pacheco D, Hahn S.** 2010. Mechanism of Mediator recruitment by tandem Gcn4 activation domains and three Gal11 activator-binding domains. Mol Cell Biol **30:**2376–2390. http://dx.doi.org/10.1128/MCB.01046-09.
24. **Thakur JK, Arthanari H, Yang F, Pan SJ, Fan X, Breger J, Frueh DP, Gulshan K, Li DK, Mylonakis E, Struhl K, Moye-Rowley WS, Cormack BP, Wagner G, Naar AM.** 2008. A nuclear receptor-like pathway regulating multidrug resistance in fungi. Nature **452:**604–609. http://dx.doi.org/10.1038/nature06836.
25. **Thakur JK, Arthanari H, Yang F, Chau KH, Wagner G, Naar AM.** 2009. Mediator subunit Gal11p/MED15 is required for fatty acid-dependent gene activation by yeast transcription factor Oaf1p. J Biol Chem **284:**4422–4428. http://dx.doi.org/10.1074/jbc.M808263200.
26. **Jedidi I, Zhang F, Qiu H, Stahl SJ, Palmer I, Kaufman JD, Nadaud PS, Mukherjee S, Wingfield PT, Jaroniec CP, Hinnebusch AG.** 2010. Acti-

vator Gcn4 employs multiple segments of Med15/Gal11, including the KIX domain, to recruit Mediator to target genes in vivo. J Biol Chem **285:**2438–2455. http://dx.doi.org/10.1074/jbc.M109.071589.
27. **Kim S, Gross DS.** 2013. Mediator recruitment to heat shock genes requires dual Hsf1 activation domains and Mediator Tail subunits Med15 and Med16. J Biol Chem **288:**12197–12213. http://dx.doi.org/10.1074/jbc.M112.449553.
28. **Taatjes DJ, Naar AM, Andel F, Nogales E, Tjian R.** 2002. Structure, function, and activator-induced conformations of the CRSP coactivator. Science **295:**1058–1062. http://dx.doi.org/10.1126/science.1065249.
29. **Cai G, Imasaki T, Takagi Y, Asturias F.** 2009. Mediator structural conservation and implications for the regulation mechanism. Structure **17:**559–567. http://dx.doi.org/10.1016/j.str.2009.01.016.
30. **Ebmeier CC, Taatjes DJ.** 2010. Activator-Mediator binding regulates Mediator-cofactor interactions. Proc Natl Acad Sci U S A **107:**11283–11288. http://dx.doi.org/10.1073/pnas.0914215107.
31. **Kremer SB, Kim S, Jeong JO, Moustafa YM, Chen A, Zhao J, Gross DS.** 2012. Role of Mediator in regulating Pol II elongation and nucleosome displacement in *Saccharomyces cerevisiae*. Genetics **191:**95–106. http://dx.doi.org/10.1534/genetics.111.135806.
32. **Takahashi H, Parmely TJ, Sato S, Tomomori-Sato C, Banks CA, Kong SE, Szutorisz H, Swanson SK, Martin-Brown S, Washburn MP, Florens L, Seidel CW, Lin C, Smith ER, Shilatifard A, Conaway RC, Conaway JW.** 2011. Human Mediator subunit MED26 functions as a docking site for transcription elongation factors. Cell **146:**92–104. http://dx.doi.org/10.1016/j.cell.2011.06.005.
33. **Donner AJ, Ebmeier CC, Taatjes DJ, Espinosa JM.** 2010. CDK8 is a positive regulator of transcriptional elongation within the serum response network. Nat Struct Mol Biol **17:**194–201. http://dx.doi.org/10.1038/nsmb.1752.
34. **Dai C, Whitesell L, Rogers AB, Lindquist S.** 2007. Heat shock factor 1 is a powerful multifaceted modifier of carcinogenesis. Cell **130:**1005–1018. http://dx.doi.org/10.1016/j.cell.2007.07.020.
35. **Mendillo ML, Santagata S, Koeva M, Bell GW, Hu R, Tamimi RM, Fraenkel E, Ince TA, Whitesell L, Lindquist S.** 2012. HSF1 drives a transcriptional program distinct from heat shock to support highly malignant human cancers. Cell **150:**549–562. http://dx.doi.org/10.1016/j.cell.2012.06.031.
36. **Scherz-Shouval R, Santagata S, Mendillo ML, Sholl LM, Ben-Aharon I, Beck AH, Dias-Santagata D, Koeva M, Stemmer SM, Whitesell L, Lindquist S.** 2014. The reprogramming of tumor stroma by HSF1 is a potent enabler of malignancy. Cell **158:**564–578. http://dx.doi.org/10.1016/j.cell.2014.05.045.
37. **Liu XD, Liu PC, Santoro N, Thiele DJ.** 1997. Conservation of a stress response: human heat shock transcription factors functionally substitute for yeast HSF. EMBO J **16:**6466–6477. http://dx.doi.org/10.1093/emboj/16.21.6466.
38. **Singh H, Erkine AM, Kremer SB, Duttweiler HM, Davis DA, Iqbal J, Gross RR, Gross DS.** 2006. A functional module of yeast Mediator that governs the dynamic range of heat-shock gene expression. Genetics **172:**2169–2184.
39. **McDaniel D, Caplan AJ, Lee MS, Adams CC, Fishel BR, Gross DS, Garrard WT.** 1989. Basal-level expression of the yeast *HSP82* gene requires a heat shock regulatory element. Mol Cell Biol **9:**4789–4798. http://dx.doi.org/10.1128/MCB.9.11.4789.
40. **Gross DS, English KE, Collins KW, Lee S.** 1990. Genomic footprinting of the yeast *HSP82* promoter reveals marked distortion of the DNA helix and constitutive occupancy of heat shock and TATA elements. J Mol Biol **216:**611–631. http://dx.doi.org/10.1016/0022-2836(90)90387-2.
41. **Giardina C, Lis JT.** 1995. Dynamic protein-DNA architecture of a yeast heat shock promoter. Mol Cell Biol **15:**2737–2744. http://dx.doi.org/10.1128/MCB.15.5.2737.
42. **Hahn JS, Hu Z, Thiele DJ, Iyer VR.** 2004. Genome-wide analysis of the biology of stress responses through heat shock transcription factor. Mol Cell Biol **24:**5249–5256. http://dx.doi.org/10.1128/MCB.24.12.5249-5256.2004.
43. **Erkine AM, Magrogan SF, Sekinger EA, Gross DS.** 1999. Cooperative binding of heat shock factor to the yeast *HSP82* promoter *in vivo* and *in vitro*. Mol Cell Biol **19:**1627–1639. http://dx.doi.org/10.1128/MCB.19.3.1627.
44. **Fan X, Chou DM, Struhl K.** 2006. Activator-specific recruitment of Mediator in vivo. Nat Struct Mol Biol **13:**117–120. http://dx.doi.org/10.1038/nsmb1049.
45. **Zhao J, Herrera-Diaz J, Gross DS.** 2005. Domain-wide displacement of histones by activated heat shock factor occurs independently of Swi/Snf and is not correlated with RNA polymerase II density. Mol Cell Biol **25:**8985–8999. http://dx.doi.org/10.1128/MCB.25.20.8985-8999.2005.
46. **Erkina TY, Tschetter PA, Erkine AM.** 2008. Different requirements of the SWI/SNF complex for robust nucleosome displacement at promoters of heat shock factor and Msn2- and Msn4-regulated heat shock genes. Mol Cell Biol **28:**1207–1217. http://dx.doi.org/10.1128/MCB.01069-07.
47. **Kremer SB, Gross DS.** 2009. SAGA and Rpd3 chromatin modification complexes dynamically regulate heat shock gene structure and expression. J Biol Chem **284:**32914–32931. http://dx.doi.org/10.1074/jbc.M109.058610.
48. **Erkina TY, Zou Y, Freeling S, Vorobyev VI, Erkine AM.** 2010. Functional interplay between chromatin remodeling complexes RSC, SWI/SNF and ISWI in regulation of yeast heat shock genes. Nucleic Acids Res **38:**1441–1449. http://dx.doi.org/10.1093/nar/gkp1130.
49. **Wang X, Sun Q, Ding Z, Ji J, Wang J, Kong X, Yang J, Cai G.** 2014. Redefining the modular organization of the core Mediator complex. Cell Res **24:**796–808. http://dx.doi.org/10.1038/cr.2014.64.
50. **Zhang F, Sumibcay L, Hinnebusch AG, Swanson MJ.** 2004. A triad of subunits from the Gal11/tail domain of Srb mediator is an in vivo target of transcriptional activator Gcn4p. Mol Cell Biol **24:**6871–6886. http://dx.doi.org/10.1128/MCB.24.15.6871-6886.2004.
51. **Li Y, Bjorklund S, Jiang YW, Kim YJ, Lane WS, Stillman DJ, Kornberg RD.** 1995. Yeast global transcriptional regulators Sin4 and Rgr1 are components of mediator complex/RNA polymerase II holoenzyme. Proc Natl Acad Sci U S A **92:**10864–10868. http://dx.doi.org/10.1073/pnas.92.24.10864.
52. **Haruki H, Nishikawa J, Laemmli UK.** 2008. The anchor-away technique: rapid, conditional establishment of yeast mutant phenotypes. Mol Cell **31:**925–932. http://dx.doi.org/10.1016/j.molcel.2008.07.020.
53. **Knop M, Siegers K, Pereira G, Zachariae W, Windsor B, Nasmyth K, Schiebel E.** 1999. Epitope tagging of yeast genes using a PCR-based strategy: more tags and improved practical routines. Yeast **15:**963–972. http://dx.doi.org/10.1002/(SICI)1097-0061(199907)15:10B<963::AID-YEA399>3.0.CO;2-W.
54. **Erkine AM, Adams CC, Diken T, Gross DS.** 1996. Heat shock factor gains access to the yeast *HSC82* promoter independently of other sequence-specific factors and antagonizes nucleosomal repression of basal and induced transcription. Mol Cell Biol **16:**7004–7017. http://dx.doi.org/10.1128/MCB.16.12.7004.
55. **Balakrishnan SK, Gross DS.** 2008. The tumor suppressor p53 associates with gene coding regions and co-traverses with elongating RNA polymerase II in an in vivo model. Oncogene **27:**2661–2672. http://dx.doi.org/10.1038/sj.onc.1210935.
56. **Pfaffl MW.** 2001. A new mathematical model for relative quantification in real-time RT-PCR. Nucleic Acids Res **29:**e45. http://dx.doi.org/10.1093/nar/29.9.e45.
57. **Andrau JC, van de Pasch L, Lijnzaad P, Bijma T, Koerkamp MG, van de Peppel J, Werner M, Holstege FC.** 2006. Genome-wide location of the coactivator Mediator: binding without activation and transient Cdk8 interaction on DNA. Mol Cell **22:**179–192. http://dx.doi.org/10.1016/j.molcel.2006.03.023.
58. **Fan X, Struhl K.** 2009. Where does Mediator bind in vivo? PLoS One **4:**e5029. http://dx.doi.org/10.1371/journal.pone.0005029.
59. **Galdieri L, Desai P, Vancura A.** 2012. Facilitated assembly of the preinitiation complex by separated tail and head/middle modules of the Mediator. J Mol Biol **415:**464–474. http://dx.doi.org/10.1016/j.jmb.2011.11.020.
60. **Jeronimo C, Robert F.** 2014. Kin28 regulates the transient association of Mediator with core promoters. Nat Struct Mol Biol **21:**449–455. http://dx.doi.org/10.1038/nsmb.2810.
61. **Paul E, Zhu ZI, Landsman D, Morse RH.** 2015. Genome-wide association of Mediator and RNA polymerase II in wild-type and Mediator mutant yeast. Mol Cell Biol **35:**331–342. http://dx.doi.org/10.1128/MCB.00991-14.
62. **Park D, Lee Y, Bhupindersingh G, Iyer VR.** 2013. Widespread misinterpretable ChIP-seq bias in yeast. PLoS One **8:**e83506. http://dx.doi.org/10.1371/journal.pone.0083506.
63. **Teytelman L, Thurtle DM, Rine J, van Oudenaarden A.** 2013. Highly expressed loci are vulnerable to misleading ChIP localization of multiple unrelated proteins. Proc Natl Acad Sci U S A **110:**18602–18607. http://dx.doi.org/10.1073/pnas.1316064110.
64. **Tsai KL, Sato S, Tomomori-Sato C, Conaway RC, Conaway JW, Astu-**

**rias FJ.** 2013. A conserved Mediator-CDK8 kinase module association regulates Mediator-RNA polymerase II interaction. Nat Struct Mol Biol **20:**611–619. http://dx.doi.org/10.1038/nsmb.2549.

65. **Moustafa Y.** 2015. Mediator is an intrinsically dynamic multisubunit complex that regulates heat shock gene transcription. Louisiana State University Health Sciences Center, Shreveport, LA.
66. **Bhaumik SR, Raha T, Aiello DP, Green MR.** 2004. *In vivo* target of a transcriptional activator revealed by fluorescence resonance energy transfer. Genes Dev **18:**333–343. http://dx.doi.org/10.1101/gad.1148404.
67. **Bhoite LT, Yu Y, Stillman DJ.** 2001. The Swi5 activator recruits the Mediator complex to the *HO* promoter without RNA polymerase II. Genes Dev **15:**2457–2469. http://dx.doi.org/10.1101/gad.921601.
68. **Leroy C, Cormier L, Kuras L.** 2006. Independent recruitment of Mediator and SAGA by the activator Met4. Mol Cell Biol **26:**3149–3163. http://dx.doi.org/10.1128/MCB.26.8.3149-3163.2006.
69. **Koschubs T, Lorenzen K, Baumli S, Sandstrom S, Heck AJ, Cramer P.** 2010. Preparation and topology of the Mediator middle module. Nucleic Acids Res **38:**3186–3195. http://dx.doi.org/10.1093/nar/gkq029.
70. **Chong YT, Koh JL, Friesen H, Duffy K, Cox MJ, Moses A, Moffat J, Boone C, Andrews BJ.** 2015. Yeast proteome dynamics from single cell imaging and automated analysis. Cell **161:**1413–1424. http://dx.doi.org/10.1016/j.cell.2015.04.051.
71. **Liu Y, Ranish JA, Aebersold R, Hahn S.** 2001. Yeast nuclear extract contains two major forms of RNA polymerase II Mediator complexes. J Biol Chem **276:**7169–7175.
72. **Lariviere L, Geiger S, Hoeppner S, Rother S, Strasser K, Cramer P.** 2006. Structure and TBP binding of the Mediator head subcomplex Med8-Med18-Med20. Nat Struct Mol Biol **13:**895–901. http://dx.doi.org/10.1038/nsmb1143.
73. **Koschubs T, Seizl M, Lariviere L, Kurth F, Baumli S, Martin DE, Cramer P.** 2009. Identification, structure, and functional requirement of the Mediator submodule Med7N/31. EMBO J **28:**69–80. http://dx.doi.org/10.1038/emboj.2008.254.